The conserved Cdc14 phosphatase ensures effective resolution of meiotic recombination intermediates.

Paula Alonso-Ramos,[1,¶] David Álvarez-Melo,[1,¶] Katerina Strouhalova,[1] Carolina Pascual-Silva,[1] George B. Garside,[2] Meret Arter,[3] Teresa Bermejo,[1] Rokas Grigaitis,[3] Rahel Wettstein,[3] Pedro San-Segundo,[4] Joao Matos,[3] Marco Geymonat,[5] Jesús A. Carballo[1,*]

[1] Department of Cellular and Molecular Biology, Centro de Investigaciones Biológicas Margarita Salas, CSIC, Ramiro de Maeztu 9, 28040, Madrid, Spain

[2] Leibniz Institute for Age Research/Fritz Lipmann Institute (FLI) Beutenbergstr. 11; D-07745 Jena; Germany

[3] Institute of Biochemistry, HPM D6.5 - ETH Zürich, Otto-Stern-Weg 3, 8093 Zürich, Switzerland

[4] Instituto de Biología Funcional y Genómica. Consejo Superior de Investigaciones Científicas and University of Salamanca. 37007-Salamanca, Spain

[5] Department of Genetics, University of Cambridge, Downing Street, Cambridge, CB2 3EH, United Kingdom

[¶] These authors contributed equally to this work

*Corresponding author: j.carballo@cib.csic.es

Abstract

Meiotic defects derived from incorrect DNA repair during gametogenesis can lead to mutations, aneuploidies and infertility. Effective and coordinated resolution of meiotic recombination intermediates is necessary to accomplish both rounds of successful chromosome segregation. Cdc14 is an evolutionarily conserved dual-specificity phosphatase required for mitotic exit and meiotic progression. Mutations that inactivate the phosphatase lead to meiotic failure. Here, we have identified previously undescribed roles of Cdc14 in ensuring correct meiotic recombination. We found that recombination intermediates accumulate during prophase I when Cdc14 is depleted. Furthermore, Cdc14 plays a role in correct homolog disjunction at the end of anaphase I, both by modulating the timely removal of arm-cohesion between sister chromatids and by promoting elimination of *SPO11*-dependent entanglements. We also demonstrate that Cdc14 is required for correct sister chromatid segregation during the second meiotic division, independent of centromeric cohesion but dependent on the correct reduplication of SPBs during meiosis II, and on the activity of the Holliday Junction resolvase Yen1/GEN1. Timely activation of Yen1/GEN1 in anaphase I and II is impaired in the meiosis defective allele, $cdc14^{3HA}$. Based on these new findings, we propose previously undescribed functions of Cdc14 in the regulation of meiotic recombination; roles that are independent of sister chromatid cohesion, spindle dynamics and the metabolism of gamete morphogenesis.

Author Summary

Meiotic recombination is fundamental for sexual reproduction, with efficient and orchestrated resolution of recombination intermediates critical for correct chromosome segregation. Homologous recombination is initiated by the introduction of programmed DNA Double-Strand Breakds (DSBs) followed by the formation of complex branched DNA intermediates, including double Holliday Junctions (dHJs). These recombination intermediates are eventually repaired into crossover or non-crossover products. In some cases, unresolved recombination intermediates, or toxic repair products, might persist until the metaphase to anaphase transition, requiring a set of late-acting repair enzymes to process them. Unrestrained activity of these enzymes, however, is equally detrimental for genome integrity, thus several layers of regulation tightly control them. For example, in budding yeast meiosis, Yen1/GEN1 is mainly activated during the second meiotic division, although how it is activated is unknown. Here, we have identified that the phosphatase Cdc14 is required during meiotic divisions for timely nuclear localization and activation of Yen1 in budding yeast meiosis. Additionally, we have been able to identify previously undescribed roles of Cdc14 in controlling meiotic recombination. Strikingly, we found that levels of recombination intermediates increase during prophase I in *cdc14* meiotic deficient cells, indicating that Cdc14 plays a direct role in monitoring meiotic DSB repair, possibly in Yen1-independent manner. Resolution of recombination intermediates in the absence of Cdc14 is dependent on *SGS1* and *MUS81/MMS4*, otherwise accumulating different types of aberrant recombination intermediates and a highly reduced efficiency in CO formation. Deficient resolution of JMs in *cdc14* meiotic cells, together with difficulties in SPB reduplication, likely contribute to the missegregation problems observed during the second meiotic division.

Introduction

Meiotic recombination is initiated by the conserved Spo11 transesterase, which introduces numerous DNA Double-Strand Breaks (DSBs) into the genome [1]. Association of single strand DNA binding proteins, including RPA, Rad51 and the meiosis specific recombinase, Dmc1, with the resected DSB ends promotes strand invasion into the intact homologous non-sister chromatid template, which culminates in the formation of a displacement loop (D-loop). Nascent D-loops can be processed through the Synthesis Dependent Strand Annealing (SDSA) repair pathway to generate non-crossover (NCO) repair products [2]. Alternatively, stabilization of the D-loop followed by second-end capture gives rise to double Holliday Junction (dHJ) intermediates. In budding yeast meiosis, dHJs are most frequently resolved into crossovers (COs) through the combined action of Mlh1-Mlh3 (MutLγ) and Exo1 [3, 4]. A second class of COs arises from the resolution of recombination intermediates via the Structure

Selective Endonuclease (SSE) Mus81/Mms4 [5]. In addition, multiple rounds of strand exchange over a stabilized D-loop, can give rise to three and four interconnected duplexes, also known as multichromatid joint molecules (mc-JMs) [6]. Further, both 3'-ends might also participate in multi-invasion events on two or three chromatids, creating heavily branched DNA structures [7]. These complex DNA species must be efficiently processed to prevent the risk of becoming potential hazards for the genome integrity due to their capacity to form aberrant crossovers, or other forms of toxic repair products. Resolution of all types of JMs requires the orchestrated action of a set of helicases and endonucleases, capable of displacing multi-branched DNA assemblies. The Bloom's syndrome helicase (BLM/Sgs1), in addition to be involved in SDSA repair, plays a prominent role in resolving aberrant "off-pathway" JMs, including mc-JMs [8-12].

It is less clear which enzymatic complexes take over the function of removing any unresolved branched DNA intermediates once meiotic cells leave the pachytene stage. Upon activation of *NDT80*-dependent transcription, and activation of the budding yeast polo-like kinase Cdc5, cells abandon the pachytene stage concomitantly with a surge of enzymatic activity that culminates in the resolution of ZMM-dependent, and independent, dHJs to give rise to COs and some NCO products [13, 14]. Cdc5 phosphorylation is required to stimulate the function of a set of SSEs, most notoriously Mus81-Mms4 [15, 16]. The Mus81-Mms4 complex acts on branched DNA substrates that have not been resolved by the canonical ZMM-dependent Class-I CO pathway [4, 10]. On the other hand, Yen1^{GEN1}, a conserved member of the Rad2/XPG family of SSEs, appears to act much later in meiosis, despite the fact that Yen1 is considered a prototypical HJ resolvase [17]. In meiotic cells, this discrepancy is easily explained since the activity of Yen1 is negatively regulated by CDK-dependent phosphorylation, preventing the activation of the nuclease during prophase I [15]. Abolition of CDK-phosphorylation in Yen1, turns on the protein's enzymatic activity prematurely and promotes its nuclear localization. Therefore, counteracting the phosphorylation of Yen1 generates the fully active form of the nuclease [15, 18]. In mitotic cells, dephosphorylation of Yen1 is carried out by the Cdc14 phosphatase [19, 20]. Activation of Yen1 during anaphase by Cdc14 allows the resolution of persistent repair intermediates that otherwise impose a physical impediment to chromosome segregation. It is currently unknown whether Cdc14 also dephosphorylates Yen1 in meiosis. Furthermore, it is unclear whether Yen1 might be briefly activated following anaphase I onset, or whether it is limited to anaphase II exclusively [4, 15].

Cdc14 is a well-conserved dual-specificity phosphatase, and it has been defined as a key component in the reversal of CDK phosphorylation during the completion of mitosis [21]. In budding yeast, Cdc14 activity is essential and cells lacking this phosphatase will remain arrested at the end of mitosis [22, 23]. Additionally, Cdc14 regulates transcriptional silencing at the rDNA, and other repeated sequences [24-26]. Several pathways regulate Cdc14 localization and activity. The RENT complex, required for transcription inhibition at the rDNA intergenic spacers (IGS), retains Cdc14 at the nucleolus until anaphase through its interaction with the Cif1/Net1 protein [27, 28]. Cdc14 is released from the nucleolus by the sequential action of two additional pathways. The FEAR (Cdc Fourteen Early

Anaphase Release) pathway promotes the early release of Cdc14 through the phosphorylation of Cif1/Net1 and Cdc14 [29-34]. Late in anaphase, the Mitotic Exit Network (MEN) keeps Cdc14 in its released state, allowing the de-phosphorylation of additional substrates, important for the full termination of mitosis and cytokinesis [35, 36].

In addition to curtailing CDK activity at the end of mitosis, Cdc14 plays critical roles promoting chromosome segregation [37]. In *S. cerevisiae*, it is required for the correct segregation of the ribosomal gene array (rDNA) and telomeres [38-40]. Lack of transcriptional silencing at these regions prevents the loading of condensins at the rDNA, and subtelomeric regions [26, 38, 41], which leads to unresolved linkages, intertwined sister chromatids, and non-disjunction during mid-anaphase. Notably, a number of functions have been allocated to Cdc14 before its anaphase-triggered release. In particular, Cdc14 has been involved in the completion of late-replicating regions in the rDNA locus, and other parts of the genome [42]. Additionally, anaphase-independent release of Cdc14 was observed upon induction of DNA damage, where generation of DSBs promoted the transitory release of Cdc14 from the nucleolus, targeting the SPB component Spc110 for dephosphorylation [43].

Cdc14 is also critically required for the completion of meiosis [44]. In budding yeast, Cdc14 is released from the nucleolus in two waves; the first during anaphase I and the second in anaphase II [45-47]. Contrary to mitotic cells, Cdc14 release from the nucleolus requires the essential function of the FEAR pathway whereas it appears that the MEN pathway is dispensable [48-50]. Additionally, some components of the MEN pathway, such as Cdc15, have functionally differentiated to fulfil a requirement in spore morphogenesis [48, 49]. Meiotic depletion of the MEN component Cdc15 leads to progression through both meiotic divisions but impairs spore formation. This meiotic function of Cdc15 appears to be independent of Cdc14 [49]. Curiously, inactivation of the FEAR pathway in meiosis allows exclusively one round of nuclear division to take place, culminating with the formation of asci carrying two diploid spores (dyads) [45, 46, 48, 51, 52].

Premature activation of FEAR blocks spindle assembly during meiosis, a process normally averted by $PP2A^{Cdc55}$ [53-55]. On the other hand, inactivation of Cdc14 function by means of FEAR mutants, or by employing conditional temperature sensitive alleles of the phosphatase, impairs the second round of chromosome segregation [45, 46]. Furthermore, absence of the phosphatase creates chromosome entanglements, a problem that can be reverted by deleting *SPO11* [46]. Occasionally, the second meiotic division takes place over a single meiosis II spindle in the absence of Cdc14 and subsequently, these cells carry out aberrant chromosome segregation [54]. These interesting observations prompted the identification of another critical function of Cdc14 at the meiosis I to meiosis II transition, which is the licensing of SPB re-duplication/half-bridge separation. Asymmetrical enrichment of Cdc14 on a single SPB during anaphase I promotes SPB re-duplication, otherwise preventing the initial step of morphogenesis of new SPBs [56].

Cdc14 is highly conserved and orthologs have been identified in other organisms, including fission yeast, nematodes, insects, and vertebrates [57]. The human genome contains three Cdc14 paralogs,

hCDC14A, hCDC14B and hCDC14C [58, 59]. Depletion of Cdc14A, required for mitotic CDK inactivation, leads to defects in centrosome duplication, mitosis and cytokinesis [60]. In vertebrates, CDC14B exits the nucleolus in response to DNA damage [61, 62], a process conserved in fission yeast [63], and more recently also observed in budding yeast [43]. Thus, in addition to playing important roles in the DNA Damage Response (DDR) [61] it appears that both Cdc14A and Cdc14B might be required for efficient repair of damaged DNA [62].

Here, we describe various previously unknown roles of Cdc14 in budding yeast. First, we reveal its direct involvement in ensuring correct meiotic recombination by suppressing the accumulation of recombination intermediates during prophase I. We also show that Cdc14 functions in resolving a subset of aberrant JMs, presumably by regulating other substrates during, or concomitantly with, the completion of prophase I. Finally, we demonstrate that Cdc14 is required for the timely activation of the conserved HJ resolvase Yen1/GEN1 during both meiotic divisions.

Results

cdc14^{3HA} is a novel meiosis-specific separation-of-function allele of *CDC14*

During the course of unrelated studies, we generated the *cdc14^{3HA}* allele carrying an endogenous C-terminal tagged version of the *CDC14* gene with three copies of the hemagglutinin epitope (3HA). Unlike other temperature sensitive alleles of *cdc14* used in many studies (see introduction), mitotic growth was not affected in diploid cells carrying the *cdc14^{3HA}* allele when grown at different temperatures on solid or liquid media (Fig 1A). Thus, we conclude that *cdc14^{3HA}* cells behave like *CDC14* at all temperatures tested under standard unchallenged growth conditions.

Unexpectedly, when homozygous SK1 background diploid *cdc14^{3HA}* cells were induced to sporulate in liquid media, very few asci that contained spores were observed. In contrast, *CDC14* control strains analyzed in parallel showed extensive tetrad formation (asci containing four spores) (Fig 1B). Following an extended incubation time in sporulation media, cells with untagged and tagged Cdc14 were sampled at 24, 48, 72, or 96 hours, fixed and analyzed under the microscope. Over 90% of cells in the *CDC14* diploid completed sporulation after 24 hours (Fig 1B). Conversely, *cdc14^{3HA}* strains displayed as few as 10% of asci containing one or two spores at all times examined (Fig 1B).

To confirm the observed defect in liquid media during sporogenesis of *cdc14^{3HA}* cells, we further induced sporulation in solid media and assessed the presence of N,N-bisformyldityrosine in the sporulated cultures. Dityrosine is a component that comprises approximately 50% of the mass of the outer spore wall layer [64]. Dityrosine is an autofluorescent molecule that possesses an excitation and emission wavelength of 325nm and 400nm respectively. Thus, when sporulated cultures are exposed under the UV^{325nm} light, spores emit visible light that can be detected using standard photographic methods (Fig 1C). *CDC14* and *cdc14^{3HA}* cells were plated on supplemented sporulation media and they were incubated for at least three days. After the incubation period, plates were directly illuminated with

both white light, and UV light and they were photographed (Fig 1C, left and right panels respectively). As anticipated, wild-type diploid strains emitted autofluorescence when exposed to UV light. On the other hand, we could not observe any UV-induced autofluorescence from *cdc14*^{3HA} diploid colonies (Fig 1C and S2B Fig). All together, we confirmed that *cdc14*^{3HA} diploid strains cannot efficiently complete sporulation despite their apparently normal mitotic growth.

Bulk DNA synthesis is not altered in *cdc14*^{3HA} mutant cells

To gain greater insight into why *cdc14*^{3HA} mutants fail to form spores, we followed different stage-specific markers to characterize the mutant phenotype in detail. First, we sought to find whether the initiation of the meiotic program was altered by studying meiotic DNA replication kinetics. During the mitotic cell cycle, released Cdc14 has been shown to de-phosphorylate replication factors, such as Sld2 and Dpb2 [65]. In addition, the lack of Cdc14 activity has been linked to problems during DNA replication termination [42]. Thus, we considered the possibility that affecting the regulatory circuit involving the Cdc14 phosphatase could cause bulk DNA replication problems during meiotic S-phase. FACS analysis of DNA content revealed that S-phase progression occurred with nearly identical kinetics in both control and *cdc14*^{3HA} strains (Fig 1D). This result suggests that initiation of meiotic S-phase is not altered in *cdc14*^{3HA} cells.

cdc14^{3HA} cells initiate both meiotic divisions

In most organisms, meiosis is characterized by a single round of DNA replication followed by two rounds of nuclear divisions [66], thus we examined whether *cdc14*^{3HA} cells were capable of separating the nuclear content during both meiotic divisions. To achieve this, synchronous cultures of *CDC14* and *cdc14*^{3HA} cells were cultured in parallel and samples were collected and fixed every two hours for at least 10-12 hours and up to 24 hours after induction of meiosis. Fixed samples were stained with 4',6-diamidino-2-phenylindole (DAPI) and counted under the fluorescence microscope for nuclear division. Results showed that *CDC14* cells initiated nuclear divisions around five hours after transfer to sporulation medium and most cells displayed more than one DAPI-stained nucleus by ten hours (Fig 1E). On the other hand, *cdc14*^{3HA} cells displayed subtly slower kinetics of nuclear divisions as well as an overall lower amount of cells exiting the one-nucleus stage by ten hours. Prolonged time-courses showed that, eventually, most *cdc14*^{3HA} cells exited the one nuclei stage, although with a ~60 min delay compared to *CDC14* control cells (Fig 1E; S1 Fig).

Previous work has shown that most cells in temperature sensitive mutants of *cdc14* complete meiosis with two nuclei, due to the inability to assemble two fully functional meiosis II spindles [44, 46, 54, 67]. Furthermore, in the very few cells that continue to the second round of chromosome segregation in *cdc14 ts* mutants, MII spindles do not assemble normally because of problems in SPB reduplication/half-bridge separation at the meiosis I-to-meiosis II transition [56]. SPB half-bridge

separation likely requires Cdc14-mediated de-phosphorylation of the SPB component Sfi1 during anaphase I [68]. However, we noticed that meiotic nuclear divisions went past the two-nuclei stage in a high proportion of *cdc14*^{3HA} cells (S1A Fig), distinguishing this *cdc14*^{3HA} allele from those temperature sensitive alleles described in earlier studies.

Next, we wanted to test whether the phenotype described for *cdc14*^{3HA} could be reproduced under other forms of meiosis-specific inactivation/depletion. To achieve this, we replaced the endogenous promoter of *CDC14* with the *CLB2* promoter, which is actively repressed in meiotic cells [69]. Cells expressing *CDC14* under the control of the *CLB2* promoter (*cdc14-md*) recapitulated the sporulation defect of *cdc14*^{3HA} (Fig 4F). Meiotic nuclear divisions took place in the *cdc14-md* but most cells remained binucleated following extended periods in meiosis (S1A Fig). Thus, the terminal meiotic phenotype of *cdc14-md* appears to be slightly different from that of *cdc14*^{3HA}.

Cdc14 protein levels are depleted during meiosis in *cdc14*^{3HA} cells

To discern the cause of the *cdc14*^{3HA} phenotype, we analyzed Cdc14^{3HA} protein levels during the entire length of meiotic time-courses. *CDC14* and *cdc14*^{3HA} cells were synchronized and induced to sporulate in parallel. Samples were collected every 2 hours and protein extracts obtained from each sample. Western blot analysis showed that *cdc14*^{3HA} cells accumulate reduced levels of the tagged protein, even at time zero, prior to meiotic induction. Levels of Cdc14^{3HA} protein become untraceable after 6-8 hours into meiosis (Fig 2A-B). To directly ascertain if Cdc14 protein levels varied from mitotically dividing cells to meiotic cells, in both the control and *cdc14*^{3HA} mutant strains, we prepared protein extracts from exponentially growing cultures. We also included the *cdc14-md* strain in our assay, to compare protein levels for all meiosis-specific mutants tested. The overall levels of Cdc14^{3HA} were lower in mitotic and meiotic dividing cells when compared to the wild type. On the other hand, Cdc14 levels in the mitotically dividing *cdc14-md* allele were similar to the wild type, and were higher than *cdc14*^{3HA} protein levels when growing exponentially (Fig 2C). Strikingly, although levels of Cdc14 were almost invariant for the wild-type strain in mitotic or meiotic cells (Exp. vs Mei$_0$), both *cdc14*^{3HA} and *cdc14-md* showed a drastic depletion with meiosis onset (Fig 2C). Finally, we compared protein levels of *cdc14*^{3HA} with those from the *cdc14-md* strains (Fig 2D). We found that depletion of Cdc14 was more effective in the *cdc14-md* allele, while in *cdc14*^{3HA} it occurred more gradually. This is not related to the ability to progress into meiosis, since all strains underwent meiotic S-phase with similar kinetics (Fig 2D; bottom panels). Currently, it is unknown to us what triggers the selective protein degradation process of the Cdc14^{3HA} phosphatase. We exclude the nature of the HA tag itself, as Smk1-3HA protein was included as internal control in our western blots, and proteins levels were stable, and even increased during mid to late meiosis (Fig 2A). Increasing the copy number of different *cdc14* alleles, as well as overproduction of the Cdc14^{3HA} protein restored sporulation (Fig 1F and S2 Fig). These results confirm that reduction of phosphatase protein levels, but not its full depletion, is causing the meiotic phenotype in the *cdc14*^{3HA}cells.

cdc14^{3HA} cells undergo two rounds of SPB duplication and separation before degenerating

Following the identification of the meiotic *cdc14^{3HA}* phenotype, we proceeded to study at the cellular and molecular level what might be preventing *cdc14^{3HA}* cells from completing sporulation when the protein levels of the phosphatase are reduced. As mentioned above, most *cdc14^{3HA}* cells eventually passed the two-nuclei stage observed as terminal meiotic phenotype in *cdc14-md* (this study) and other *cdc14* temperature sensitive mutants [44, 46, 67]. Thus, we monitored the kinetics and morphology of the meiotic SPBs and spindles during the first and the second divisions. Both *CDC14* and *cdc14^{3HA}* cells, carrying GFP-tubulin and Spc29-CFP to visualize spindles and SPBs respectively, were induced to undergo synchronous meiosis. Samples were then collected and studied under the microscope at times where MI, MII, and later stages in the sporogenic process take place [70-72]. In addition to the kinetics of nuclear divisions, the number of SPBs per individual cell were counted. Cells with two or more Spc29-CFP foci were considered to have initiated one or both meiotic divisions (Fig 2E-F; S3A Fig). This was confirmed by the presence of linearly distributed bundles of microtubules characteristic of the meiotic spindle (Fig 2E). Furthermore, nuclear segregation was monitored simultaneously by looking at the separation of SPB-associated DAPI masses (Fig 2F). We observed that by eight hours into meiosis, *CDC14* and *cdc14^{3HA}* cultures contained around 75% and 60% of cells with more than one SPB, respectively. Among the population of cells that showed multiple SPBs, 56% of wild-type cells presented more than two Spc29 foci; therefore, they had initiated meiosis II. However, only 40% of *cdc14^{3HA}* cells displayed more than two Spc29 foci, confirming a slight reduction of cells forming meiosis II spindles carrying four SPBs. This observation correlates with the slightly lower frequency of *cdc14^{3HA}* cells containing more than two DAPI masses (Fig 2F; S1A Fig). As expected, after 24 hours of meiotic induction, wild-type *CDC14* cells showed over 90% of cells with three or four SPBs. In marked contrast, the *cdc14^{3HA}* meiotic mutant possessed more than two thirds of cells lacking a single Spc29-CFP focus, suggesting that in the absence of Cdc14 the structural integrity of SPBs becomes compromised once meiotic divisions take place (Fig 2F; S3 Fig). On the other hand, parallel studies using the *cdc14-md* showed cells with 2 SPBs, 3 at most, for the full length of the time-course (S3D Fig), confirming the earlier studies revealing the role for the phosphatase in SPB reduplication [56].

Meiotic spindle dynamics are not altered in the *cdc14^{3HA}* mutant

Since we found that SPB re-duplication and separation was not fully impeded in the *cdc14^{3HA}* mutant, along with the fact that we could detect cells past the second nuclear division, we investigated whether the observed SPBs assembled functional spindles at both MI and MII. In addition, we assessed if the kinetics of both chromosomal divisions were altered in the mutant. To test that, wild-type and *cdc14^{3HA}* strains carrying Tub1-GFP and Spc29-CFP were induced to undergo meiosis synchronously and at appropriate times, they were transferred to an incubator chamber for image acquisition using live-cell

microscopy (Fig 3A-B; S1 and S2 Video). To analyze the first meiotic division, the time between metaphase I and the end of telophase I was recorded. Thus, for *CDC14* cells, the MI spindle extension-to-breakage period lasted around 53 min under our experimental conditions. Cells from the *cdc14*^{3HA} culture completed MI in 58 min, on average, which was not statistically different from control cells (Fig 3C). Next, we estimated the length of MII by timing the period between metaphase II spindles and the lengthening of the microtubule bundles until the tubulin signal became diffuse (Fig 3B). The average length of MII divisions was 80 min and 86 min for *CDC14* and *cdc14*^{3HA} cells, respectively (Fig 3C). Taken together, we conclude that the detected reduction in Cdc14^{3HA} abundance throughout meiosis affected neither the lifespan, nor dynamic, of meiosis I and meiosis II spindles.

cdc14^{3HA} cells undergo stepwise loss of meiotic cohesins at key meiotic transitions with minimal delay

In previous studies, thermal inactivation of Cdc14 in meiosis led to a small delay in the loss of both arm and centromeric cohesion upon anaphase I onset [46]. To test whether *cdc14*^{3HA} mutant cells displayed similar behaviour, we followed the stepwise loss of Rec8-GFP from chromosomes throughout the entire meiotic cycle by time-lapse microscopy (Fig. 3D-E). During prophase I, Rec8 localized at chromosome arms until metaphase I (Fig 3E-F). Disappearance of nuclear Pds1/Securin signal was used as a marker of anaphase I entry. Following Pds1 degradation, most anaphase I cells lost Rec8-GFP signal from the chromosomes in both wild type and *cdc14*^{3HA}. Among those cells, ~75% of wild-type cells displayed pericentromeric Rec8-GFP enrichment and 25% displayed diffused, albeit still chromatin associated Rec8-GFP signal (Fig 3D-F). 30 minutes after anaphase I onset, 50% of wild-type cells still displayed pericentromeric signal and the remaining 50% were lacking Rec8-GFP signal completely. By 60 minutes past anaphase I, >85% of cells displayed no Rec8-GFP signal and less than 15% still displayed pericentromeric Rec8 (Fig 3F). On the other hand, *cdc14*^{3HA} cells displayed analogous stepwise loss of cohesins as the wild type did, however, ~40% of mutant cells displayed pericentromeric Rec8-GFP signal, which was ~35% less than in wild type, whereas ~60% of *cdc14*^{3HA} cells displayed diffused Rec8-GFP signal still associated with the chromatin. After 30 minutes into anaphase I, ~50% of mutant cells displayed pericentromeric Rec8 signal, a comparable frequency to the observed in the wild type. The remaining 50% of cells showed no detectable Rec8-GFP signal, matching the frequencies displayed by the wild type at the same time point. After 60 minutes following anaphase I, ~25% of mutant cells displayed pericentromeric Rec8, which was moderately higher than for the wild type (Fig 3F). Altogether, *cdc14*^{3HA} cells are able of undergoing stepwise cohesin loss at key transitions during meiosis, although with slightly reduced efficiency in comparison to the wild type.

cdc14^{3HA} mutants missegregate sister chromatids during meiosis II

While monitoring late meiotic events in *cdc14*^{3HA} mutants, we observed a high frequency of cells with more than four nuclei (S1B and S3C Figs). This might be due to impediments during chromosome

segregation in the first and/or the second division. To test this possibility, we analyzed the nuclear morphology, along with the meiotic spindle, in individual cells undergoing the first and second divisions (Fig 4A-B). Cells presenting a meiosis I (MI) spindles with a length of ≥5µm were considered to be in late anaphase I, and therefore, two DAPI masses should be distinguishable. On the other hand, cells presenting DAPI-stained bridges at the end of anaphase I might reflect those cells with some form of chromosome entanglement [46].

Wild-type cells showed clear separation of nuclear content in 74% of the anaphases analyzed, and only ~25% of anaphase I cells presented DAPI-stained bridges (Fig 4A). By contrast, *cdc14*^{3HA} cells had only ~20% fully resolved two nuclei after anaphase I. ~80% of *cdc14*^{3HA} mutant anaphase cells presented some kind of chromosomal bridge, suggesting that despite having undergone MI spindle elongation correctly, some form of DNA entwining was not properly resolved. Similar results were observed for the *cdc14-md* allele, where ~80% of anaphase I cells showed entanglements (Fig 4A).

The observed anaphase I bridges could be due to transitory entanglement of lagging, under-condensed chromosomal domains, that could be eventually resolved before the initiation of the second meiotic division. Furthermore, a subtle delay in cohesin removal was observed in *cdc14*^{3HA} anaphase I cells (Fig 3F), which might be responsible, for at least a fraction of these bridged DAPI masses. To test if the anaphase I bridges were eventually eliminated or persisted until the second meiotic division, we looked at metaphase II cells and scored the configuration of their nuclear masses (Fig 4B). The wild type presented over 76% of metaphase II cells with single individualized nuclei located within each MII spindle. By contrast, 75% of metaphase II cells in the *cdc14*^{3HA} mutant showed DNA threads connecting both nuclear masses. Strikingly, we were unable to detect metaphase II cells with 4-SPBs for the *cdc14-md* mutant, thus we could not perform such analysis in this background. The severity of the SPB re-duplication/half-bridge separation phenotype in this mutant seems to be more drastic than it is observed for the *cdc14*^{3HA} mutant allele.

We conclude that diminished levels of Cdc14 in meiosis results in the abnormal formation of nuclear bridges after the first meiotic division and that these bridges persist at least until metaphase II.

To determine whether the DNA bridges present at metaphase II in *cdc14* mutant cells are the consequence or the cause of other problems arising during chromosome segregation, we constructed strains carrying fluorescent markers on specific chromosomes and followed their segregation [73]. We made use of *tetO* repeats integrated at the interstitial *lys2* locus of chromosome II, together with the presence of the *tetR* repressor gene fused with GFP, which associates to these repeats [74, 75]. A second strain with a different GFP reporter was made, but in this case, it carried *lacO* repeats in a centromere-proximal region at the *trp1* locus of chromosome IV, with a *lacI* repressor gene fused to GFP integrated at the *ura3* locus [76]. First, we analyzed strains carrying *LYS2-GFP* on both homologs to determine chromosome segregation fidelity in cells that had completed both meiotic divisions. In this way, we were able to visualize four individual dots segregating to each of the four nuclei within a single tetranucleated cell. The results showed that chromosome II segregated correctly in 95% of wild-type

cells. Notably, only 78% of *cdc14*^{3HA} tetranucleated cells presented the correct GFP distribution, whereas the remaining 22% of mutant cells displayed, at least, one of the four nuclei lacking a GFP focus (Fig 4C; S4 Fig). To understand the origin of chromosome missegregation in the *cdc14*^{3HA} cells we further analyzed the first and the second division separately. In order to determine correct homolog disjunction, we first analyzed binucleated cells using strains carrying the *CENIV-GFP* tag in homozygosity (S5A Fig). We found that the *cdc14*^{3HA} mutation did not enhance missegregation of homologs during the first meiotic division (Fig 4D). Very similar results were previously reported for homozygous *CENV-GFP* in *cdc14-1* mutants [54]. Next, we analyzed sister chromatid segregation in the second meiotic division. Thus, heterozygous strains for the *CENIV-GFP* marker were used; 79% of wild-type cells showed correct sister separation after meiosis II. In contrast, 50% of tetranucleated *cdc14*^{3HA} cells displayed problems segregating sister centromeres (Fig 4E). Taken all together, we conclude that accurate sister chromatid segregation in meiosis requires unperturbed Cdc14 activity.

The absence of meiotic recombination partially alleviates the sporulation defect of *cdc14*^{3HA}

We considered that the increase in sister chromatid missegregation after the second division in *cdc14*^{3HA} cells could be in part originated from aberrant recombination causing entanglements between sister chromatids. If this is the case, we should be able to alleviate some of the sporulation problems associated to the *cdc14*^{3HA} mutation by eliminating meiotic recombination. To test this hypothesis we combined the *cdc14*^{3HA} allele with the *spo11* mutation, which prevents DSB formation [1]. The absence of DSBs improved the separation of DAPI mases in anaphase I in the *cdc14*^{3HA} mutant (Fig 4A). Therefore, recombination leads to the formation of anaphase I bridges in *cdc14*^{3HA} strains. Intriguingly, sister missegregation after meiosis II could not be tested in the *spo11 cdc14*^{3HA} double mutant because the SPB re-duplication defect, previously described, was highly aggravated [56].

On the other hand, the sporulation defect was partially rescued in all combinations of *spo11* with *cdc14* meiotic-defective mutants tested (Fig 4F).

Meiotic recombination is impaired in *cdc14*^{3HA} mutants

Elimination of Spo11-dependent DSBs robustly alleviates problems with homologous chromosome segregation in FEAR mutants or in a *cdc14-1* background [46]. We have confirmed this rescue by introducing *spo11* deficiency in *cdc14*^{3HA} and *cdc14-md* mutants (Fig 4A and 4F). Thus, it seems that Cdc14 could play a role in promoting accurate repair of Spo11-dependent DSBs. To gain greater insight into the function of Cdc14 during meiotic recombination, we analyzed the well-studied *HIS4::LEU2* (*HIS4-LEU2*) meiotic recombination hotspot (Fig 5A; [77-80]) in the presence of the *cdc14*^{3HA} and *cdc14-md* mutations. First, we analyzed total levels of DSBs, CO and NCOs products (Fig 5B-D). Levels of DSBs and COs were very similar in the three strains. In contrast, *cdc14*^{3HA} and *cdc14-md*

mutants showed a small reduction in NCO levels in comparison to the wild-type strain (Fig 5C-D). Furthermore, we noticed a slower turnover of DNA species of higher molecular weight, corresponding with branched recombination intermediates [6] (Fig 5A and 5E). To distinguish whether the accumulation of these intermediates was due to slower turnover or increased formation of those branched species, we studied their abundance in the *ndt80Δ* mutant background, where resolution of JMs is largely prevented due to the lack of *CDC5*-dependent JM-resolution promoting activity [14]. Surprisingly, levels of high molecular weight species accumulated twice as much in the *cdc14*^{3HA} mutant over the wild type (Fig 5F and 5H). This unbalanced JM accumulation was accompanied by moderately higher levels of DSBs in the *cdc14*^{3HA} mutant. In contrast, no differences in NCO levels was observed in the *ndt80Δ* background between the two strains (Fig 5G-H). Thus, *CDC14* appears to counteract the accumulation of a population of high molecular-weight intermediates of recombination during, or before, prophase I.

Next, we wondered how the higher levels of JMs originated in the mutant. For that, we examined earlier recombination intermediates by 2D-gel analysis using the same hotspot (Fig 6A and S6 Fig). Different DNA species were quantified at two different time points from synchronous meiotic *ndt80Δ* cultures. Results confirmed that the total levels of JMs were increased in the *cdc14*^{3HA} and the *cdc14-md* mutants, with respect to the wild-type strain (Fig. 6B-C and S6 Fig).

We wanted to monitor if the resolution stage of DSB repair could also be affected in *cdc14* mutants, and not just the initial accumulation of recombination intermediates. Since *cdc14* mutants already presented abnormally high levels of JMs in *ndt80Δ* background over the *CDC14 ndt80Δ* wild-type version (Fig. 5H and 6C), we decided to evaluate the efficiency of JM resolution in a *mus81Δ* mutant background, where total levels of JMs were similar in both *mus81Δ ndt80Δ* and *mus81Δ cdc14 ndt80Δ* mutant combinations (S6B-C Fig). After 7 hours in SPM, *CDC5* expression, by means of β-estradiol (ES) addition to the media [14], allowed us to follow the efficiency of recombination intermediates resolution into CO and NCO products, in both *mus81Δ* and *mus81Δ cdc14*^{3HA} mutants (Fig 6D-E). Induced expression of *CDC5* in the *mus81Δ* mutant efficiently led to the formation of COs, only one hour after ES addition to the medium. CO levels did not increase further after the 8-hour time-point. NCOs, on the other hand, steadily increased reaching their maximum at 17 hours in SPM+ES (24h). In contrast, fewer COs were detected one hour after *CDC5* induction in the presence of *cdc14*^{3HA} mutation, and final levels did not increase at the end of the 24-hour time-course. NCOs levels were also lower in comparison to the *mus81Δ* mutant background alone, and total levels did not rise over the period when *CDC5* was expressed (Fig 6E). Thus, it appears that when comparable levels of JMs accumulate, Cdc14 could be required for efficient formation of COs and NCOs, at least when meiotic DSB-repair takes place in a *mus81Δ* mutant background. To confirm that Cdc14 plays a relevant role in the late resolution of repair intermediates, we decided to study the efficiency of repair in a *NDT80* background. To this end, we took advantage of the well-known negative effect on DSB-repair when depleting Sgs1 in combination with mutations in one or more of the SSEs like *mms4/mus81* and *yen1*/*slx1*/*slx4* [4, 10].

Strikingly, the *cdc14-md sgs1-md mms4* triple mutant displayed very high levels of unrepaired JMs after 24 hours in meiosis in comparison to the *sgs1-md mms4* double mutant alone (Fig 6F). Total JMs in *cdc14-md sgs1-md mms4* accumulated to analogous levels as in the *sgs1-md mms4 yen1* triple mutant (Fig 6G). Furthermore, the reduced formation of COs in the *sgs1-md mms4 cdc14* strain was also nearly identical to the one observed for the triple mutant *sgs1-md mms4 yen1* (Fig 6H-I).

Thus, Cdc14 is required for proper processing of recombination intermediates. These results also suggest that the chromosome non-disjunction events observed in *FEAR*, *cdc14-1, and cdc14-md* mutants ([45, 46]; this study), as well as the sister chromatid missegregation in *cdc14*^{3HA} mutants, may be a consequence, at least in part, of the abnormal accumulation and processing of Spo11-dependent JMs in the absence of Cdc14 activity.

Yen1 nuclear localization and activity requires full levels of Cdc14 activity

The Cdc14 requirement for the correct processing of meiotic JMs led us to search for suitable candidates that could be regulated by the phosphatase in meiosis. We have determined that the absence of Cdc14 leads to similar defects in JM processing and repair that the absence of Yen1 (Fig. 6F-I). Additionally, Yen1 has been described as a target of Cdc14 in mitotic cells [19, 20, 81]. Thus, to determine whether Yen1 could be a target of Cdc14 during meiosis, we first tested the subcellular localization of Yen1, which is known to change in a phosphorylation-dependent and cell-cycle stage-specific manner, both in mitotic and meiotic cells [15]. In mitotic cells, Yen1 localization is cytoplasmic when CDK activity is high, but it enters the nucleus upon anaphase onset. Cdc14 release in anaphase reverts CDK-dependent phosphorylation of the endonuclease, allowing the un-phosphorylated Yen1 to enter the nucleus at this stage [19, 20, 81]. We tested Yen1 localization once cells initiated anaphase I and found that nuclear Yen1 was more infrequent in *cdc14*^{3HA} mutants than it was in wild type (Fig 7A). This result indicates that Yen1 nuclear localization is reduced in the presence of *cdc14*^{3HA} mutation. We also tested if the activity of the nuclease changed during a meiotic time-course in the *cdc14*^{3HA} mutant (Fig 7B-C). Samples were collected every two hours from synchronized meiotic cultures of wild-type and *cdc14*^{3HA} cells, each of them carrying a functional tagged version of the *YEN1* gene fused to 9 copies of the *MYC* epitope [18]. From each time-point, Yen1-9Myc was immunoprecipitated from the meiotic extracts and beads carrying the protein were incubated with a synthetic Holliday Junction substrate [82]. Active Yen1 should be able to cleave the HJ substrate whereas the phosphorylated inactive form of the nuclease would not. In wild-type diploid cells, Yen1-9myc did not display significant nuclease activity during early stages of the meiotic time course, prior to the accumulation of Cdc5, except for the residual endonuclease activity observed at t=0 hours (Fig 7B). Approximately 2 hr after the accumulation of Cdc5, we detected robust HJ processing, consistent with activation of Yen1 at late stages of meiosis (Fig 7B-C; [15]). Notably, the resolvase activity displayed by Yen1 in *cdc14*^{3HA} cultures was extremely low for the duration of the time course (Fig 7B-C). Meiotic S-phase was completed with similar timing in wild-type and *cdc14* cells suggesting that both strains were transiting at similar kinetics through the

time course (Fig 7D). Moreover, the Cdc5 protein (marking the exit from prophase I) was detected at the same time and at the same levels in both wild-type and *cdc14* cultures (Fig. 7B). Thus, these results strongly suggest that Cdc14 promotes nuclear accumulation of Yen1 during anaphase I and is required for its enzymatic activity at late stages of meiosis.

Constitutively active Yen1 supresses the accumulation of aberrant recombination intermediates in *cdc14^{3HA}* mutants

Next, we sought to eliminate the requirement of Cdc14 phosphatase for Yen1 activation by directly using a phosphorylation-resistant version of the nuclease (*YEN1^{ON}*). Mutation of nine of the CDK consensus sites of phosphorylation in Yen1 renders the protein constitutively active [18, 20]. We combined the *cdc14^{3HA}* allele with *YEN1^{ON}* and tested for sporulation efficiency. Similar to the elimination of Spo11-dependent DSBs, unrestrained activity of Yen1 partly rescued the sporulation defect of *cdc14^{3HA}* (Fig 7E). Since enhanced sporulation efficiency might not necessarily reflect improved chromosome segregation (Fig. 4), we directly tested the effect of *YEN1^{ON}* in chromosome segregation during both meiotic divisions (Fig 7F). First, we checked if the presence of Yen1^{ON} would help resolving DAPI-stained DNA bridges observed at late anaphase I in *cdc14^{3HA}* mutants. Indeed, a two-fold improvement over *cdc14^{3HA}* single mutants was observed. Furthermore, missegregation of sister chromatids was fully rescued to the levels of *YEN1^{ON}* single mutant in the *cdc14^{3HA} YEN1^{ON}* double mutant in comparison to the *cdc14^{3HA}* single mutant (Fig 7F). Moreover, to confirm if the improvement in chromosome segregation by *YEN1^{ON}* was due to the restoration of Yen1's nuclease activity, we tested this possibility using a resolution assay in a *cdc14^{3HA}* mutant background (Fig 7G). Unlike Yen1^{WT}, Yen1^{ON} displayed potent resolvase activity in the absence of Cdc14 activity. Altogether, by eliminating the requirement for Cdc14 in de-phosphorylating Yen1, we partly rescue the chromosome missegregation defect and the lack of resolvase activity observed in *cdc14^{3HA}* mutants, confirming that Yen1 activation by Cdc14 is important for late resolution of toxic recombination intermediates.

Discussion

Meiotic recombination is fundamental for sexual reproduction, ensuring that homologous chromosomes segregate correctly at the first meiotic division as well as to facilitate distinct allele combinations that sustain evolution. Homologous recombination is initiated by the introduction of programmed DSBs followed by homolog pairing and DNA strand exchange. Those early steps in the recombination process lead to the formation of stable JMs, which are ultimately resolved into two main classes of HR repair products, known as COs and NCOs (Fig 8). Recombining chromosomes may also contain intermediates consisting of three- and four-armed DNA structures such as mc-JMs, where three and four DNA duplexes stay connected (Fig 8; [8, 9, 79, 83-87]). In some cases, unresolved recombination

intermediates might persist until the metaphase to anaphase transition where a subset of late-acting nucleases process them in order to safeguard genome integrity [88]. Unrestrained activity of such nucleases can interfere with the correct allotment of COs and NCOs in meiosis [18], thus, they are tightly controlled by several layers of regulation. Posttranslational modifications carried out principally by key cell cycle kinases, like CDK, DDK, and PLK1, are the most extended form of regulation [15, 16]. Additionally, at least one of the late acting nucleases, Yen1, has been described to be modulated through the highly conserved Cdc14 phosphatase in mitotic cells [19, 20, 81]. Given the essentiality of *CDC14* in *S. cerevisiae*, most meiotic studies performed to date have required the use of conditional temperature sensitive alleles of *cdc14* that cannot complete meiosis following the first round of chromosome segregation [22, 46, 56, 67]. Despite the large amount of valuable data that has been collected over the past years using these alleles, other less conspicuous functionalities of Cdc14, particularly those affecting meiosis II, might have been precluded from being discovered when studying meiosis in *cdc14 ts* mutants. Here, using two different meiotic-deficient alleles of *CDC14* we have been able to identify previously undetected functions of the phosphatase during meiosis, particularly those affecting the second meiotic division (Fig 8). Furthermore, we found the unprecedented requirement of *CDC14* to prevent the accumulation of JMs during meiotic prophase I, as well as for their repair, suggesting that Cdc14 regulates other not yet identified enzymatic activities that are required for the early resolution of these branched molecules. Unexpectedly, deletion of *MUS81* led to similar accumulation of JMs as in the absence of *CDC14* or in the double mutant *mus81Δ cdc14*^{3HA} (S6 Fig). It is tempting to speculate that Cdc14 might directly, or indirectly, modulate earlier roles of the Mus81-Mms4 complex in meiosis by preventing aberrant JM accumulation in prophase I. Future studies might help to address such possibility.

Novel insights into Cdc14 functionalities by using an epitope-tagged version of the phosphatase

In the present work we describe an allele of *CDC14* (*cdc14*^{3HA}) that displays no obvious defects during unchallenged mitotic divisions; nonetheless, it is strongly deficient in sporulation during meiosis. *cdc14*^{3HA} is a C-terminal tagged version of *CDC14* with three copies of hemagglutinin, which has been used in other studies to monitor its behaviour during mitosis [27, 33, 36] and meiosis [50]. Protein levels of the phosphatase are severely reduced in homozygous *cdc14*^{3HA} meiotic cells (Fig 2A-D), a problem also perceived during the mitotic cell cycle, although not as dramatic. No such problems have been reported when 3xHA is fused at the N-terminal end of Cdc14 ([46]; this study), or when *cdc14*^{3HA} is present in heterozygosity together with the wild-type *CDC14* allele [89], making this phenotype exclusive for the C-terminally tagged version of the gene. *cdc14*^{3HA} mutant cells complete meiotic DNA replication and both nuclear divisions with kinetics similar to those of the wild type, suggesting that both rounds of chromosome segregation take place in *cdc14*^{3HA} meiotic cells. Nonetheless, the *cdc14*^{3HA} mutant fails to form spores once cells completed both nuclear divisions. We exclude that the process

which initiates spore formation was affected since we visualized pro-spore membrane components and found them to appear with similar kinetics in the mutant strain as they did in the wild type (S7 Fig). Other groups have also described similar defects in sporulation in the absence of Cdc14 activity, or components of the MEN pathway [49, 90]. Critical for our findings was to detect correct SPB re-duplication and separation in a high proportion of *cdc14*^{3HA} cells, but not in the more restrictive *cdc14-md* strain (Fig 2E-F; S3 Fig). Furthermore, many *cdc14*^{3HA} cells were able to assemble functional tetrapolar spindles at metaphase/anaphase II confirming that problems arising in the *cdc14*^{3HA} mutant somewhat differ from those in the *cdc14-md* as well as in the widely employed, thermo-sensitive alleles, *cdc14-1, -3* or other FEAR mutants [46, 54, 56]. One possibility is that differences in the mechanism by which Cdc14 activity is depleted during meiosis might be responsible for the observed variations in the meiotic behaviour. Even so, most of the described phenotypical features regarding the recombination-dependent missegregation are reproduced for *cdc14*^{3HA} (Fig 4), so our allele recapitulates those impaired functionalities linked to the recombination defect previously observed. Notwithstanding, meiotic divisions occur in most *cdc14*^{3HA} cells with no discernible delay in spindle dynamics when compared to wild-type cells (Fig 3A-C). A very subtle delay, observed during both divisions, could in part arise from difficulties in SPB re-duplication and half-bridge separation, as described in *cdc14-1* cells [56]. Similarly, inactivation of Cdc14 in cells transiting metaphase II, did not show any effect on the lifetime of meiosis II spindles [90], confirming that the phenotype we observe can be reproduced under different modes of Cdc14 inactivation during meiosis. Moreover, the meiotic delays observed in *cdc14*^{3HA} are not restricted to the completion of meiotic divisions. A short delay in cohesin removal from the chromosome to the pericentromeric region was also detected when entering anaphase I (Fig 3D-F). Rec8 clearance from meiotic chromosomes had been previously reported to be inefficient in *spo12*, *slk19* and *cdc14-1* mutants [46]. Thus, *cdc14*^{3HA} shares this particular meiotic phenotype with other alleles of *cdc14* in regards to stepwise kinetics of cohesin loss. It is possible that delayed Rec8 removal from chromosomes could contribute to the presence of DNA bridges in late anaphase I. However, it is worth mentioning that the frequencies of *cdc14*^{3HA} cells presenting anaphase I bridges is consistently higher than those cells displaying persistent Rec8 signal during anaphase I (Figs 3F and 4A), thus it is unlikely that inefficient Rec8 removal is the only source of most DNA bridges, but instead a contributing factor. This possibility is still compatible with a *SPO11*-dependent formation of entanglements. Further experiments will need to be performed to unveil the complex nature of these DAPI structures appearing in late anaphase I in certain mutants. Strikingly, levels of sister chromatids missegregation, but not of homologs, are substantial once *cdc14*^{3HA} cells entered the second meiotic division, suggesting that residual unresolved recombination intermediates could affect sister chromatid disjunction more acutely than that of homologs. These results again highlight the importance of safeguarding correct genome repair during the entire length of the meiotic cell cycle. Non-disjunction at either first or second division could likewise bring severe consequences to the correct ploidy of the developing gametes.

CDC14-dependent resolution of recombination intermediates via multiple mechanisms

The appearance of most types of JMs should occur from zygotene until the end of pachytene stage [80], far earlier than the first release of Cdc14 at anaphase I that has been reported during meiosis. Nevertheless, this is not the first time that the requirement of Cdc14 has been linked to cell cycle stages that precedes its bulk release from the nucleolus. Cdc14 has been involved in completion of late-replicating regions in the rDNA, and other parts of the genome. Such problems arise due to insufficient dosage of replication factors, although those deficiencies in principle seemed to be contingent on the reduced Cdc14 activity in preceding mitoses in the *cdc14-1* allele used for such study [42]. Notwithstanding, collision amidst transcription and replication due to absence of Cdc14-mediated transcriptional silencing during S-phase is expected also to hamper the completion of DNA replication. Irrespectively, the insufficient dosage of replication factors in *cdc14* cells stems from two main reasons: i) nuclear import is constitutively impaired in *cdc14* cells, preventing essential replication factors to enter into the nucleus properly, such is the case for certain subunits of RPA; and ii) reduced transcription of genes controlled by MBF and SBF transcription complexes in G1 which translates into reduced protein levels. Furthermore, Swi6, a transcription factor member of MBF and SCF complexes, requires the de-phosphorylation of its phospho-Serine 160 by Cdc14, in order to be imported to the nucleus upon mitotic exit [91]. Swi6 has also been shown to be important in meiotic cells [92] and the expression of genes like *RAD54* and *RAD51* is downregulated in a *swi6* mutant. Furthermore, intragenic recombination frequencies between *his4-4* and *his4-290* is considerably decreased in the *swi6* mutant, suggesting that the earlier accumulation of JMs might be the consequence of a reduced dosage of recombination proteins. By extrapolation, the defective processing of recombination intermediates observed at the *HIS4-LEU2* recombination hotspot in *cdc14*^{3HA} mutant might be the consequence of the reduced activity of the Cdc14^{3HA} phosphatase during previous mitotic divisions before entering into meiosis, given the reduced levels of phosphatase displayed in this mutant also in cycling cells (Fig 2C). Nonetheless, a *cdc14-md* mutant did not display reduced protein levels in mitotic cultures while still manifested high levels of JMs in prophase I. Thus, it appears unlikely that problems arising outside meiosis would cause this abnormal accumulation of JMs. In contrast, we favour a role of Cdc14 in the direct regulation of substrates required for correct processing of JMs in prophase I [4, 10, 15]. Interestingly, the conserved SSE, Yen1^{GEN1} is a critical substrate of Cdc14 during budding yeast mitosis, and it exhibits a phosphorylation-regulated nucleocytoplasmic shuttling behaviour similar to that of Swi6 [93]. Namely, CDK-dependent phosphorylation restricts Yen1 from entering the nucleus and becoming active, whereas reversal of that phosphorylation by Cdc14 allows Yen1 to enter the nucleus and resolve entangled DNA-structures [19, 20, 81]. Nonetheless, Yen1 nuclear import and activation appears to be concomitant with bulk Cdc14 release from the nucleolus during anaphase. This is why a role for Yen1 in safeguarding chromosome segregation has been proposed, especially, during the second meiotic division. Our results support such a conclusion, since higher frequencies of aneuploidies

and missegregation are detected during meiosis II for a *cdc14*^{3HA} meiotic mutant (Fig 4E). This is consistent with the demonstrated ability of Cdc14 to activate Yen1 (Fig 7A-C). Puzzlingly, the residual resolvase activity of Yen1 observed at time=0 in wild-type meiotic cultures might reflect certain level of early functionality (Fig 7B-C), perhaps important for the repair of any residual DNA damage carried over from the preceding mitosis. Such early resolvase activity is not observed in *cdc14*^{3HA} mutants (Fig 7B-C). Taking into account that the levels of JMs in *mus81Δ ndt80Δ*-arrested cells are similar to those observed in *cdc14 ndt80Δ* mutants (S6 Fig), it is possible that SSEs play important functions in processing "off pathway" JMs generated as consequence of secondary DNA damage, which might be unrelated to *SPO11*-induced DNA repair. Such mechanisms could safeguard genome integrity at both, beginning and end, of meiosis putting Yen1 and Cdc14 as part of a specialized surveillance repair pathway that ensures DSB-repair fidelity, while preventing that other sources of unrepaired secondary damage to interfere with the canonical inter-homolog recombination repair. Whether or not Yen1 acts during anaphase I is less clear. Nuclear localization of Yen1 is moderately high at anaphase I (Fig 7A) and maximal during anaphase II [18], but its endonucleolytic activity is only extensively turned on once MII spindles appear ([18]; Fig 7C). Perhaps, minimal nuclear localization does not necessarily boost Yen1 activity, which might require additional regulatory modifications only present at the second stage of meiotic divisions [94]. Interestingly, it has been shown that Cdc14 only gets fully released to the cytoplasm during the second meiotic division, whereas the first division confines Cdc14 diffusion within just the nucleoplasm [47].

Absence of Cdc14 activity in cells depleted for *SGS1* and *MMS4* displayed the same recombination problems as the triple mutant *sgs1 mms4 yen1* (Fig 6F-I). Additionally, unrestrained action of Yen1 (Yen1^{ON}) restores faithful chromosome segregation and resolvase activity in *cdc14*^{3HA} diploid cells. Furthermore, Yen1^{ON} partly restores sporulation in both *cdc14* mutants. Considering all the observations mentioned above, we conclude that the lack of Yen1 activity is somewhat responsible, but not entirely, for the severity of the *cdc14*^{3HA} meiotic phenotype.

Additional meiosis-specific substrates of Cdc14 during gametogenesis.

It has been known for some time that *cdc14* and FEAR mutants display problems segregating chromosomes in a *SPO11*-dependent way [45, 46]. Consistently, the *cdc14*^{3HA} sporulation and homolog nondisjunction defects are somewhat solved when eliminating Spo11 activity (Fig 4).

Recombination at the rDNA does not occur during meiotic prophase I [95], a process actively inhibited due to the exclusion of Hop1 from the nucleolus [96-98]}. Thus, difficulties segregating this region do not seem to be the origin of the *SPO11*-dependent entanglements. Nonetheless, absence of chiasmata might partly alleviate the segregation impediments in chromosome 12 caused by other recombination-independent roles of Cdc14 on the rDNA. Alternatively, a number of DNA-repair proteins present at the nucleolus early in prophase I might require the action of Cdc14 *in situ* in order for these enzymes, or their activities, to spread outside the rDNA. Such a role of Cdc14 directly in the nucleolus would aid

processing the presence of an excessive number of JMs generated as part of homologous recombination repair endeavours, without compromising the allotment of enzymes essential for correct rDNA functionality.

Alternatively, multiple possible nuclear substrates required for JM resolution might be required to participate, either during the transition from the pachytene stage to metaphase I, or during anaphase I upon bulk release of the phosphatase from the nucleolus. The first scenario would better suit the timing for the resolution of most JMs and it might require early release of Cdc14, or a subpopulation of the phosphatase, a possibility that to our knowledge has not been reported yet for meiotic cells. Strikingly, DNA damage caused in vegetative cells triggers the transitory release of Cdc14 from the nucleolus to the nucleoplasm, allowing the phosphatase to act on components of the SPBs and to stabilize them at metaphase [43]. Additionally, sub-populations of Cdc14 have been observed at different subcellular structures during mitosis and meiosis, including kinetochores, bud neck and SPBs/centrosomes [56, 99, 100]. In budding yeast meiosis, the timing of JM resolution and CO formation is coordinated with cell-cycle progression through the *NDT80*-dependent expression of the Polo-like kinase Cdc5 [13-15]. Thus unlike in mitotic cells, an earlier requirement of Cdc5 for the resolution of dHJ at the pachytene to MI transition, upon Ndt80 activation, might too impinge on its ability to interact with Cdc14 and Cif1/Net1 in the nucleolus. Such interaction might counteract temporally the negative regulatory effect of $PP2A^{Cdc55}$ allowing some Cdc14 molecules to escape from its captor [43, 53, 54]. Cdc5 might also play a relevant role during meiosis in promoting the early-release of a population of Cdc14 at the transition from the pachytene stage to metaphase I in order to modulate the activity of a number of safeguarding enzymes required for correct chromosome segregation. Further studies will be required to determine whether that last possibility is true.

In recent years, human orthologs of Cdc14 phosphatase have received increased attention due to their involvement in key processes like DDR, DNA repair and cell cycle control. Furthermore, recent findings point to recessive variants of the phosphatase to be directly responsible of human diseases, like deafness and male infertility [101]. Thus, in order to comprehend the underlying factors that trigger those conditions, a deeper understanding of the genetic and molecular mechanisms that are responsible for the countless functionalities of the Cdc14 phosphatase during gametogenesis and HR repair will be required.

Materials and Methods

Yeast strains and plasmids

All strains were SK1, as detailed in S1 Table. Standard yeast manipulation procedures and growth media were utilized. To introduce the 3HA tag at the C-terminal end of Cdc14, the CDC14ha3-$pKan^R$ plasmid containing the last ~500bps of the *CDC14* gene, was cloned in frame with 3xHA using the NotI restriction site, and containing the *CLB1* terminator was used. The plasmid was linearized using a

unique restriction site located within the *CDC14* sequence and transformed into a SK1 haploid strain. Alternatively, *CDC14* was tagged using the PCR-based method described in [102] using the plasmid pFA6a-3HA-kanMX6. The phenotype of *CDC14-3HA* strains obtained from both tagging methods was checked and the sporulation defect was identical. Transformants containing correct tag integration were identified and tested by western blot for the presence of the tag. Southern blot analysis and/or PCR was performed to confirm the integration at the endogenous locus. Multi-copy plasmids used in S2 Fig. were originally described in [103].

Synchronous meiotic time courses

Induction of synchronous meiosis was carried out according to the established protocols for standard assays [104]. All pre-growth and meiotic time courses were carried out at 30ºC unless specified otherwise. For *cdc14-1* meiosis, the culture was kept at 23ºC and shifted to 30ºC 2 hours after transferring into sporulation medium (SPM). Aliquots were removed at the specified times, and subjected to various analyses.

DNA manipulation, extraction and southern blot detection

Standard DNA extraction was performed as in [105]. For studies at the *HIS4-LEU2* recombination hotspot, the protocol described in [106] was followed. For 2D gel agarose electrophoresis, cell cultures were photo-crosslinked with trioxalen (Merck) using long-wave UV light before DNA extraction, in order to visualize recombination intermediates by standard southern blotting techniques at the *HIS4-LEU2* hotspot [106].

Time-lapse imaging, immunofluorescence, microscopy, and image analysis

Time-lapse experiments were performed as in [107], with small variations. In brief, 1 ml aliquots from synchronous meiotic cultures were taken at specific times, diluted 1:9 in fresh SPM (kept at 30ºC). 300µl of diluted cells were placed in suitable multi-well slides (80821 uncoated, ibidi). Slides were placed in a temperature-controlled incubation chamber from a Multidimensional Microscopy System Leica AF6000 LX. Images were taken at multiple positions and channels every 5, 10 or 15 minutes, depending on the experiment. Image acquisition was carried out using a CCD Hamamatsu 9100-02 camera. The system was controlled by the proprietary software, Leica Application Suite X, version 3.30. For preparations of fixed cells and immunofluorescence, aliquots were fixed and prepared as described in [105] and [18], respectively. Chromosomal DNA was stained with 1µg/ml 4,6-diamino-2-phenylimide (DAPI). Images were recorded and analyzed using a Deltavision (DV3) workstation from Applied Precision Inc. with a Photometrics CoolSnap HQ (10-20MHz) air cooled CCD camera and controlled by SoftWorx image acquisition and deconvolution software.

Protein extraction, Western blot analysis and antibodies

Whole-cell extracts were prepared from cell suspensions in 20% trichloroacetic acid by agitation with glass beads. Precipitated proteins were solubilized in SDS-PAGE sample buffer, and appropriate dilutions were analyzed by SDS-PAGE and western blotting. Antibodies used for western blotting were mouse monoclonal anti-MYC (1:1000, Abcam), mouse monoclonal anti-HA (1:1000) from S. Ley (NIMR)), rabbit polyclonal anti-Ssp1 (1:100) from M. Knop, goat polyclonal anti-Cdc14 (yE-17; 1:1000; Santa Cruz Biotechnology), goat polyclonal anti-Cdc5 (1:1000; Santa Cruz Biotechnology), mouse monoclonal anti-Pgk1 (1:5000; Invitrogen), goat anti-mouse IgG conjugated to horseradish peroxidase (1:10000; Sigma-Aldrich), and chicken anti-rabbit IgG conjugated to horseradish peroxidase (1:10000; Sigma-Aldrich).

Nuclease assays

For nuclease assays, myc9-tagged Yen1 and Yen1^{ON} were immuno-affinity purified from yeast using anti-Myc agarose beads (9E10) and washed extensively. The beads (approx. volume 10 µl) were then mixed with 10 µl cleavage buffer (50 mM Tris-HCl pH 7.5, 3 mM $MgCl_2$) and 15 ng of 5'-Cy3-end-labeled synthetic Holliday junction X0 DNA. After 1 h incubation at 37ºC with gentle rotation, reactions were stopped by addition of 2.5 µl of 10 mg/ml proteinase K and 2% SDS, followed by incubation for 30 min at 37ºC. Loading buffer (3 µl) was then added and fluorescently-labelled products were separated by 10% native PAGE and analyzed using a Typhoon scanner and ImageQuant software. Resolution activity was calculated by determining the fraction of nicked duplex DNA product relative to the sum of the intact substrate and resolution product. The protein input was estimated by western blot.

Data analysis and Biostatistics

Data was compiled and analyzed using Excel, LibreOffice Calc, and SPSS Statistical Data Editor. For multiple comparisons, analysis of variance (one-way ANOVA) was performed. For pairwise comparisons, two-tailed unpaired *t*-tests were used using IBM SPSS Statistics and SigmaPlot.

Acknowledgements

We would like to thank C.R. Vázquez de Aldana, M. Knop, E. Winter, A.M. Neiman, E. Hoffmann, J.L. Santos, G.V. Börner, A. Marston, M.G. Blanco and F. Machín for kindly providing us with reagents, strains, antibodies and/or advice. We are especially thankful to the Molecular Biology of the Chromosome lab in CIB for sharing lab space, reagents and equipment. We would like to thank to the microscopy facility at the CIB for valuable technical advice in designing and analysing time-lapse, to P. Jalón for UV photography acquisition and to J.S. Ahuja, for advice in 2D gel experiments.

References

1. Keeney S, Giroux CN, Kleckner N. Meiosis-specific DNA double-strand breaks are catalyzed by Spo11, a member of a widely conserved protein family. Cell. 1997;88(3):375-84. PubMed PMID: 9039264; PubMed Central PMCID: PMC9039264.

2. Bishop DK. Multiple mechanisms of meiotic recombination. Cell. 2006;127(6):1095-7. Epub 2006/12/19. doi: S0092-8674(06)01533-9 [pii]

10.1016/j.cell.2006.11.029. PubMed PMID: 17174887.

3. Zakharyevich K, Ma Y, Tang S, Hwang PY, Boiteux S, Hunter N. Temporally and biochemically distinct activities of Exo1 during meiosis: double-strand break resection and resolution of double Holliday junctions. Mol Cell. 2010;40(6):1001-15. Epub 2010/12/22. doi: S1097-2765(10)00922-6 [pii]

10.1016/j.molcel.2010.11.032. PubMed PMID: 21172664; PubMed Central PMCID: PMC3061447.

4. Zakharyevich K, Tang S, Ma Y, Hunter N. Delineation of joint molecule resolution pathways in meiosis identifies a crossover-specific resolvase. Cell. 2012;149(2):334-47. Epub 2012/04/17. doi: S0092-8674(12)00399-6 [pii]

10.1016/j.cell.2012.03.023. PubMed PMID: 22500800; PubMed Central PMCID: PMC3377385.

5. de los Santos T, Loidl J, Larkin B, Hollingsworth NM. A role for *MMS4* in the processing of recombination intermediates during meiosis in *Saccharomyces cerevisiae*. Genetics. 2001;159(4):1511-25. Epub 2002/01/10. PubMed PMID: 11779793; PubMed Central PMCID: PMC1461921.

6. Oh SD, Lao JP, Hwang PY, Taylor AF, Smith GR, Hunter N. BLM ortholog, Sgs1, prevents aberrant crossing-over by suppressing formation of multichromatid joint molecules. Cell. 2007;130(2):259-72. Epub 2007/07/31. doi: 10.1016/j.cell.2007.05.035. PubMed PMID: 17662941; PubMed Central PMCID: PMCPMC2034285.

7. Piazza A, Wright WD, Heyer WD. Multi-invasions Are Recombination Byproducts that Induce Chromosomal Rearrangements. Cell. 2017;170(4):760-73 e15. Epub 2017/08/07. doi: 10.1016/j.cell.2017.06.052. PubMed PMID: 28781165; PubMed Central PMCID: PMCPMC5554464.

8. Oh SD, Lao JP, Taylor AF, Smith GR, Hunter N. RecQ helicase, Sgs1, and XPF family endonuclease, Mus81-Mms4, resolve aberrant joint molecules during meiotic recombination. Mol Cell. 2008;31(3):324-36. Epub 2008/08/12. doi: S1097-2765(08)00467-X [pii]

10.1016/j.molcel.2008.07.006. PubMed PMID: 18691965; PubMed Central PMCID: PMC2587322.

9. Jessop L, Lichten M. Mus81/Mms4 endonuclease and Sgs1 helicase collaborate to ensure proper recombination intermediate metabolism during meiosis. Mol Cell. 2008;31(3):313-23. Epub 2008/08/12. doi: S1097-2765(08)00423-1 [pii]

10.1016/j.molcel.2008.05.021. PubMed PMID: 18691964; PubMed Central PMCID: PMC2584117.

10. De Muyt A, Jessop L, Kolar E, Sourirajan A, Chen J, Dayani Y, et al. BLM helicase ortholog Sgs1 is a central regulator of meiotic recombination intermediate metabolism. Mol Cell. 2012;46(1):43-53. Epub 2012/04/17. doi: S1097-2765(12)00207-9 [pii]

10.1016/j.molcel.2012.02.020. PubMed PMID: 22500736; PubMed Central PMCID: PMC3328772.

11. Xaver M, Huang L, Chen D, Klein F. Smc5/6-Mms21 prevents and eliminates inappropriate recombination intermediates in meiosis. PLoS Genet. 2013;9(12):e1004067. Epub 2014/01/05. doi: 10.1371/journal.pgen.1004067. PubMed PMID: 24385936; PubMed Central PMCID: PMCPMC3873250.

12. Copsey A, Tang S, Jordan PW, Blitzblau HG, Newcombe S, Chan AC, et al. Smc5/6 coordinates formation and resolution of joint molecules with chromosome morphology to ensure meiotic divisions. PLoS Genet. 2013;9(12):e1004071. Epub 2014/01/05. doi: 10.1371/journal.pgen.1004071. PubMed PMID: 24385939; PubMed Central PMCID: PMCPMC3873251.

13. Clyne RK, Katis VL, Jessop L, Benjamin KR, Herskowitz I, Lichten M, et al. Polo-like kinase Cdc5 promotes chiasmata formation and cosegregation of sister centromeres at meiosis I. Nat Cell Biol. 2003;5(5):480-5. Epub 2003/04/30. doi: 10.1038/ncb977. PubMed PMID: 12717442.

14. Sourirajan A, Lichten M. Polo-like kinase Cdc5 drives exit from pachytene during budding yeast meiosis. Genes Dev. 2008;22(19):2627-32. Epub 2008/10/04. doi: 10.1101/gad.1711408. PubMed PMID: 18832066; PubMed Central PMCID: PMCPMC2559907.

15. Matos J, Blanco MG, Maslen S, Skehel JM, West SC. Regulatory control of the resolution of DNA recombination intermediates during meiosis and mitosis. Cell. 2011;147(1):158-72. Epub 2011/10/04. doi: S0092-8674(11)01002-6 [pii]

10.1016/j.cell.2011.08.032. PubMed PMID: 21962513.

16. Wild P, Susperregui A, Piazza I, Dorig C, Oke A, Arter M, et al. Network Rewiring of Homologous Recombination Enzymes during Mitotic Proliferation and Meiosis. Mol Cell. 2019;75(4):859-74.e4. Epub 2019/07/29. doi: 10.1016/j.molcel.2019.06.022. PubMed PMID: 31351878; PubMed Central PMCID: PMCPMC6715774.

17. Ip SCY, Rass U, Blanco MG, Flynn HR, Skehel JM, West SC. Identification of Holliday junction resolvases from humans and yeast. Nature. 2008;456(7220):357-61. doi: http://www.nature.com/nature/journal/v456/n7220/suppinfo/nature07470_S1.html.

18. Arter M, Hurtado-Nieves V, Oke A, Zhuge T, Wettstein R, Fung JC, et al. Regulated Crossing-Over Requires Inactivation of Yen1/GEN1 Resolvase during Meiotic Prophase I. Dev Cell. 2018;45(6):785-800.e6. Epub 2018/06/20. doi: 10.1016/j.devcel.2018.05.020. PubMed PMID: 29920281; PubMed Central PMCID: PMCPMC6043783.

19. Eissler CL, Mazon G, Powers BL, Savinov SN, Symington LS, Hall MC. The Cdk/cDc14 module controls activation of the Yen1 holliday junction resolvase to promote genome stability. Mol Cell. 2014;54(1):80-93. Epub 2014/03/19. doi: 10.1016/j.molcel.2014.02.012. PubMed PMID: 24631283; PubMed Central PMCID: PMCPMC3988236.

20. Blanco MG, Matos J, West SC. Dual control of Yen1 nuclease activity and cellular localization by Cdk and Cdc14 prevents genome instability. Mol Cell. 2014;54(1):94-106. Epub 2014/03/19. doi: 10.1016/j.molcel.2014.02.011. PubMed PMID: 24631285; PubMed Central PMCID: PMCPMC3988869.

21. Visintin R, Craig K, Hwang ES, Prinz S, Tyers M, Amon A. The phosphatase Cdc14 triggers mitotic exit by reversal of Cdk-dependent phosphorylation. Mol Cell. 1998;2(6):709-18. Epub 1999/01/14. PubMed PMID: 9885559.

22. Culotti J, Hartwell LH. Genetic control of the cell division cycle in yeast. 3. Seven genes controlling nuclear division. Exp Cell Res. 1971;67(2):389-401. Epub 1971/08/01. PubMed PMID: 5097524.

23. Hartwell LH, Mortimer RK, Culotti J, Culotti M. GENETIC CONTROL OF THE CELL DIVISION CYCLE IN YEAST: V. GENETIC ANALYSIS OF *cdc* MUTANTS. Genetics. 1973;74(2):267-86.

24. Machín F, Torres-Rosell J, De Piccoli G, Carballo JA, Cha RS, Jarmuz A, et al. Transcription of ribosomal genes can cause nondisjunction. J Cell Biol. 2006;173(6):893-903. doi: 10.1083/jcb.200511129. PubMed PMID: 16769819; PubMed Central PMCID: PMC16769819.

25. Clemente-Blanco A, Mayan-Santos M, Schneider DA, Machin F, Jarmuz A, Tschochner H, et al. Cdc14 inhibits transcription by RNA polymerase I during anaphase. Nature. 2009;458(7235):219-22. Epub 2009/01/23. doi: 10.1038/nature07652. PubMed PMID: 19158678; PubMed Central PMCID: PMCPMC4445138.

26. Clemente-Blanco A, Sen N, Mayan-Santos M, Sacristan MP, Graham B, Jarmuz A, et al. Cdc14 phosphatase promotes segregation of telomeres through repression of RNA polymerase II transcription. Nat Cell Biol. 2011;13(12):1450-6. Epub 2011/10/25. doi: 10.1038/ncb2365. PubMed PMID: 22020438; PubMed Central PMCID: PMCPMC3232454.

27. Shou W, Seol JH, Shevchenko A, Baskerville C, Moazed D, Chen ZW, et al. Exit from mitosis is triggered by Tem1-dependent release of the protein phosphatase Cdc14 from nucleolar RENT complex. Cell. 1999;97(2):233-44. Epub 1999/04/29. PubMed PMID: 10219244.

28. Visintin R, Hwang ES, Amon A. Cfi1 prevents premature exit from mitosis by anchoring Cdc14 phosphatase in the nucleolus. Nature. 1999;398(6730):818-23. Epub 1999/05/11. doi: 10.1038/19775. PubMed PMID: 10235265.

29. Yoshida S, Toh-e A. Budding yeast Cdc5 phosphorylates Net1 and assists Cdc14 release from the nucleolus. Biochem Biophys Res Commun. 2002;294(3):687-91. Epub 2002/06/12. doi: 10.1016/s0006-291x(02)00544-2. PubMed PMID: 12056824.

30. Visintin R, Stegmeier F, Amon A. The role of the polo kinase Cdc5 in controlling Cdc14 localization. Mol Biol Cell. 2003;14(11):4486-98. Epub 2003/10/11. doi: 10.1091/mbc.e03-02-0095. PubMed PMID: 14551257; PubMed Central PMCID: PMCPMC266767.

31. Azzam R, Chen SL, Shou W, Mah AS, Alexandru G, Nasmyth K, et al. Phosphorylation by cyclin B-Cdk underlies release of mitotic exit activator Cdc14 from the nucleolus. Science. 2004;305(5683):516-9. Epub 2004/07/27. doi: 10.1126/science.1099402. PubMed PMID: 15273393.

32. Queralt E, Lehane C, Novak B, Uhlmann F. Downregulation of PP2A(Cdc55) phosphatase by separase initiates mitotic exit in budding yeast. Cell. 2006;125(4):719-32. Epub 2006/05/23. doi: 10.1016/j.cell.2006.03.038. PubMed PMID: 16713564.

33. Rahal R, Amon A. The Polo-like kinase Cdc5 interacts with FEAR network components and Cdc14. Cell Cycle. 2008;7(20):3262-72. Epub 2008/10/18. doi: 10.4161/cc.7.20.6852. PubMed PMID: 18927509; PubMed Central PMCID: PMCPMC2665935.

34. Rodriguez-Rodriguez JA, Moyano Y, Jativa S, Queralt E. Mitotic Exit Function of Polo-like Kinase Cdc5 Is Dependent on Sequential Activation by Cdk1. Cell reports. 2016;15(9):2050-62. Epub 2016/05/24. doi: 10.1016/j.celrep.2016.04.079. PubMed PMID: 27210759.

35. Stegmeier F, Visintin R, Amon A. Separase, polo kinase, the kinetochore protein Slk19, and Spo12 function in a network that controls Cdc14 localization during early anaphase. Cell. 2002;108(2):207-20. Epub 2002/02/08. PubMed PMID: 11832211.

36. Visintin C, Tomson BN, Rahal R, Paulson J, Cohen M, Taunton J, et al. APC/C-Cdh1-mediated degradation of the Polo kinase Cdc5 promotes the return of Cdc14 into the nucleolus. Genes Dev. 2008;22(1):79-90. Epub 2008/01/04. doi: 10.1101/gad.1601308. PubMed PMID: 18172166; PubMed Central PMCID: PMCPMC2151016.

37. Hartwell LH, Smith D. Altered fidelity of mitotic chromosome transmission in cell cycle mutants of *S. cerevisiae*. Genetics. 1985;110(3):381-95. Epub 1985/07/01. PubMed PMID: 3894160; PubMed Central PMCID: PMCPMC1202570.

38. D'Amours D, Stegmeier F, Amon A. Cdc14 and condensin control the dissolution of cohesin-independent chromosome linkages at repeated DNA. Cell. 2004;117(4):455-69. Epub 2004/05/13. PubMed PMID: 15137939.

39. Sullivan M, Higuchi T, Katis VL, Uhlmann F. Cdc14 phosphatase induces rDNA condensation and resolves cohesin-independent cohesion during budding yeast anaphase. Cell. 2004;117(4):471-82. Epub 2004/05/13. PubMed PMID: 15137940.

40. Torres-Rosell J, Machin F, Jarmuz A, Aragon L. Nucleolar segregation lags behind the rest of the genome and requires Cdc14p activation by the FEAR network. Cell Cycle. 2004;3(4):496-502. Epub 2004/03/09. PubMed PMID: 15004526.

41. Wang BD, Yong-Gonzalez V, Strunnikov AV. Cdc14p/FEAR pathway controls segregation of nucleolus in *S. cerevisiae* by facilitating condensin targeting to rDNA chromatin in anaphase. Cell Cycle. 2004;3(7):960-7. Epub 2004/06/11. PubMed PMID: 15190202; PubMed Central PMCID: PMCPMC2673102.

42. Dulev S, de Renty C, Mehta R, Minkov I, Schwob E, Strunnikov A. Essential global role of *CDC14* in DNA synthesis revealed by chromosome underreplication unrecognized by checkpoints in *cdc14* mutants. Proc Natl Acad Sci U S A. 2009;106(34):14466-71. Epub 2009/08/12. doi: 10.1073/pnas.0900190106. PubMed PMID: 19666479; PubMed Central PMCID: PMCPMC2723162.

43. Villoria MT, Ramos F, Duenas E, Faull P, Cutillas PR, Clemente-Blanco A. Stabilization of the metaphase spindle by Cdc14 is required for recombinational DNA repair. EMBO J. 2017;36(1):79-101. Epub 2016/11/18. doi: 10.15252/embj.201593540. PubMed PMID: 27852625; PubMed Central PMCID: PMCPMC5210157.

44. Sharon G, Simchen G. Mixed segregation of chromosomes during single-division meiosis of *Saccharomyces cerevisiae*. Genetics. 1990;125(3):475-85. Epub 1990/07/01. PubMed PMID: 2199318; PubMed Central PMCID: PMCPMC1204075.

45. Buonomo SB, Rabitsch KP, Fuchs J, Gruber S, Sullivan M, Uhlmann F, et al. Division of the nucleolus and its release of *CDC14* during anaphase of meiosis I depends on separase, *SPO12*, and SLK19. Dev Cell. 2003;4(5):727-39. Epub 2003/05/10. PubMed PMID: 12737807.

46. Marston AL, Lee BH, Amon A. The Cdc14 phosphatase and the FEAR network control meiotic spindle disassembly and chromosome segregation. Dev Cell. 2003;4(5):711-26. Epub 2003/05/10. doi: S1534580703001308 [pii]. PubMed PMID: 12737806.

47. Yellman CM, Roeder GS. Cdc14 Early Anaphase Release, FEAR, Is Limited to the Nucleus and Dispensable for Efficient Mitotic Exit. PLoS One. 2015;10(6):e0128604. Epub 2015/06/20. doi: 10.1371/journal.pone.0128604. PubMed PMID: 26090959; PubMed Central PMCID: PMCPMC4474866.

48. Kamieniecki RJ, Liu L, Dawson DS. FEAR but not MEN genes are required for exit from meiosis I. Cell Cycle. 2005;4(8):1093-8. Epub 2005/06/23. PubMed PMID: 15970684.

49. Pablo-Hernando ME, Arnaiz-Pita Y, Nakanishi H, Dawson D, del Rey F, Neiman AM, et al. Cdc15 is required for spore morphogenesis independently of Cdc14 in *Saccharomyces cerevisiae*.

Genetics. 2007;177(1):281-93. Epub 2007/07/31. doi: 10.1534/genetics.107.076133. PubMed PMID: 17660551; PubMed Central PMCID: PMCPMC2013696.

50. Attner MA, Amon A. Control of the mitotic exit network during meiosis. Mol Biol Cell. 2012;23(16):3122-32. Epub 2012/06/22. doi: 10.1091/mbc.E12-03-0235. PubMed PMID: 22718910; PubMed Central PMCID: PMCPMC3418307.

51. Kamieniecki RJ, Shanks RM, Dawson DS. Slk19p is necessary to prevent separation of sister chromatids in meiosis I. Curr Biol. 2000;10(19):1182-90. Epub 2000/10/26. doi: S0960-9822(00)00723-5 [pii]. PubMed PMID: 11050386.

52. Zeng X, Saunders WS. The Saccharomyces cerevisiae centromere protein Slk19p is required for two successive divisions during meiosis. Genetics. 2000;155(2):577-87. Epub 2000/06/03. PubMed PMID: 10835382; PubMed Central PMCID: PMC1461122.

53. Kerr GW, Sarkar S, Tibbles KL, Petronczki M, Millar JB, Arumugam P. Meiotic nuclear divisions in budding yeast require PP2A(Cdc55)-mediated antagonism of Net1 phosphorylation by Cdk. J Cell Biol. 2011;193(7):1157-66. Epub 2011/06/22. doi: jcb.201103019 [pii]

10.1083/jcb.201103019. PubMed PMID: 21690311; PubMed Central PMCID: PMC3216327.

54. Bizzari F, Marston AL. Cdc55 coordinates spindle assembly and chromosome disjunction during meiosis. J Cell Biol. 2011;193(7):1213-28. Epub 2011/06/22. doi: 10.1083/jcb.201103076. PubMed PMID: 21690308; PubMed Central PMCID: PMCPMC3216325.

55. Nolt JK, Rice LM, Gallo-Ebert C, Bisher ME, Nickels JT. PP2A (Cdc)(5)(5) is required for multiple events during meiosis I. Cell Cycle. 2011;10(9):1420-34. Epub 2011/04/02. doi: 15485 [pii]. PubMed PMID: 21455032.

56. Fox C, Zou J, Rappsilber J, Marston AL. Cdc14 phosphatase directs centrosome re-duplication at the meiosis I to meiosis II transition in budding yeast. Wellcome open research. 2017;2:2. Epub 2017/01/31. doi: 10.12688/wellcomeopenres.10507.2. PubMed PMID: 28133632; PubMed Central PMCID: PMCPMC5266553.

57. Mocciaro A, Schiebel E. Cdc14: a highly conserved family of phosphatases with non-conserved functions? J Cell Sci. 2010;123(Pt 17):2867-76. Epub 2010/08/20. doi: 10.1242/jcs.074815. PubMed PMID: 20720150.

58. Li L, Ernsting BR, Wishart MJ, Lohse DL, Dixon JE. A family of putative tumor suppressors is structurally and functionally conserved in humans and yeast. J Biol Chem. 1997;272(47):29403-6. Epub 1997/12/31. PubMed PMID: 9367992.

59. Rosso L, Marques AC, Weier M, Lambert N, Lambot MA, Vanderhaeghen P, et al. Birth and rapid subcellular adaptation of a hominoid-specific *CDC14* protein. PLoS Biol. 2008;6(6):e140. Epub 2008/06/13. doi: 10.1371/journal.pbio.0060140. PubMed PMID: 18547142; PubMed Central PMCID: PMCPMC2422853.

60. Trautmann S, McCollum D. Cell cycle: new functions for Cdc14 family phosphatases. Curr Biol. 2002;12(21):R733-5. Epub 2002/11/07. PubMed PMID: 12419203.

61. Bassermann F, Frescas D, Guardavaccaro D, Busino L, Peschiaroli A, Pagano M. The Cdc14B-Cdh1-Plk1 axis controls the G2 DNA-damage-response checkpoint. Cell. 2008;134(2):256-67. Epub 2008/07/30. doi: 10.1016/j.cell.2008.05.043. PubMed PMID: 18662541; PubMed Central PMCID: PMCPMC2591934.

62. Mocciaro A, Berdougo E, Zeng K, Black E, Vagnarelli P, Earnshaw W, et al. Vertebrate cells genetically deficient for Cdc14A or Cdc14B retain DNA damage checkpoint proficiency but are impaired in DNA repair. J Cell Biol. 2010;189(4):631-9. Epub 2010/05/19. doi: 10.1083/jcb.200910057. PubMed PMID: 20479464; PubMed Central PMCID: PMCPMC2872905.

63. Diaz-Cuervo H, Bueno A. Cds1 controls the release of Cdc14-like phosphatase Flp1 from the nucleolus to drive full activation of the checkpoint response to replication stress in fission yeast. Mol Biol Cell. 2008;19(6):2488-99. Epub 2008/04/04. doi: 10.1091/mbc.E07-08-0737. PubMed PMID: 18385517; PubMed Central PMCID: PMCPMC2397296.

64. Briza P, Winkler G, Kalchhauser H, Breitenbach M. Dityrosine is a prominent component of the yeast ascospore wall. A proof of its structure. J Biol Chem. 1986;261(9):4288-94. PubMed PMID: 3512567.

65. Bloom J, Cross FR. Novel role for Cdc14 sequestration: Cdc14 dephosphorylates factors that promote DNA replication. Mol Cell Biol. 2007;27(3):842-53. Epub 2006/11/23. doi: 10.1128/mcb.01069-06. PubMed PMID: 17116692; PubMed Central PMCID: PMCPMC1800703.

66. Zickler D, Kleckner N. Recombination, Pairing, and Synapsis of Homologs during Meiosis. Cold Spring Harb Perspect Biol. 2015;7(6). Epub 2015/05/20. doi: 10.1101/cshperspect.a016626. PubMed PMID: 25986558; PubMed Central PMCID: PMCPMC4448610.

67. Schild D, Byers B. Diploid spore formation and other meiotic effects of two cell-division-cycle mutations of *Saccharomyces cerevisiae*. Genetics. 1980;96(4):859-76. Epub 1980/12/01. PubMed PMID: 7021319; PubMed Central PMCID: PMCPMC1219305.

68. Avena JS, Burns S, Yu Z, Ebmeier CC, Old WM, Jaspersen SL, et al. Licensing of yeast centrosome duplication requires phosphoregulation of sfi1. PLoS Genet. 2014;10(10):e1004666. Epub 2014/10/24. doi: 10.1371/journal.pgen.1004666. PubMed PMID: 25340401; PubMed Central PMCID: PMCPMC4207612.

69. Lee BH, Amon A. Role of Polo-like kinase *CDC5* in programming meiosis I chromosome segregation. Science. 2003;300(5618):482-6. Epub 2003/03/29. doi: 10.1126/science.1081846

1081846 [pii]. PubMed PMID: 12663816.

70. Moens PB, Rapport E. Spindles, spindle plaques, and meiosis in the yeast *Saccharomyces cerevisiae* (Hansen). J Cell Biol. 1971;50(2):344-61. Epub 1971/08/01. PubMed PMID: 5112645; PubMed Central PMCID: PMC2108272.

71. Neiman AM. Prospore membrane formation defines a developmentally regulated branch of the secretory pathway in yeast. J Cell Biol. 1998;140(1):29-37. Epub 1998/02/14. PubMed PMID: 9425151; PubMed Central PMCID: PMCPMC2132592.

72. Knop M, Strasser K. Role of the spindle pole body of yeast in mediating assembly of the prospore membrane during meiosis. EMBO J. 2000;19(14):3657-67. Epub 2000/07/19. doi: 10.1093/emboj/19.14.3657. PubMed PMID: 10899120; PubMed Central PMCID: PMC313968.

73. Straight AF, Belmont AS, Robinett CC, Murray AW. GFP tagging of budding yeast chromosomes reveals that protein-protein interactions can mediate sister chromatid cohesion. Curr Biol. 1996;6(12):1599-608. Epub 1996/12/01. PubMed PMID: 8994824.

74. Michaelis C, Ciosk R, Nasmyth K. Cohesins: Chromosomal Proteins that Prevent Premature Separation of Sister Chromatids. Cell. 1997;91(1):35-45. doi: https://doi.org/10.1016/S0092-8674(01)80007-6.

75. Katis VL, Lipp JJ, Imre R, Bogdanova A, Okaz E, Habermann B, et al. Rec8 phosphorylation by casein kinase 1 and Cdc7-Dbf4 kinase regulates cohesin cleavage by separase during meiosis. Dev Cell. 2010;18(3):397-409. doi: 10.1016/j.devcel.2010.01.014. PubMed PMID: 20230747; PubMed Central PMCID: PMCPMC2994640.

76. Shonn MA, McCarroll R, Murray AW. Spo13 protects meiotic cohesin at centromeres in meiosis I. Genes Dev. 2002;16(13):1659-71. Epub 2002/07/09. doi: 10.1101/gad.975802. PubMed PMID: 12101124; PubMed Central PMCID: PMCPMC186364.

77. Cao L, Alani E, Kleckner N. A pathway for generation and processing of double-strand breaks during meiotic recombination in *S. cerevisiae*. Cell. 1990;61(6):1089-101. Epub 1990/06/15. doi: 0092-8674(90)90072-M [pii]. PubMed PMID: 2190690.

78. Schwacha A, Kleckner N. Identification of joint molecules that form frequently between homologs but rarely between sister chromatids during yeast meiosis. Cell. 1994;76(1):51-63. PubMed PMID: 8287479; PubMed Central PMCID: PMC8287479.

79. Hunter N, Kleckner N. The single-end invasion: an asymmetric intermediate at the double-strand break to double-holliday junction transition of meiotic recombination. Cell. 2001;106(1):59-70. PubMed PMID: 11461702; PubMed Central PMCID: PMC11461702.

80. Börner GV, Kleckner N, Hunter N. Crossover/noncrossover differentiation, synaptonemal complex formation, and regulatory surveillance at the leptotene/zygotene transition of meiosis. Cell. 2004;117(1):29-45. PubMed PMID: 15066280; PubMed Central PMCID: PMC15066280.

81. Garcia-Luis J, Clemente-Blanco A, Aragon L, Machin F. Cdc14 targets the Holliday junction resolvase Yen1 to the nucleus in early anaphase. Cell Cycle. 2014;13(9):1392-9. Epub 2014/03/15. doi: 10.4161/cc.28370. PubMed PMID: 24626187; PubMed Central PMCID: PMCPMC4050137.

82. Grigaitis R, Susperregui A, Wild P, Matos J. Characterization of DNA helicases and nucleases from meiotic extracts of *S. cerevisiae*. Methods Cell Biol. 2018;144:371-88. Epub 2018/05/29. doi: 10.1016/bs.mcb.2018.03.029. PubMed PMID: 29804678.

83. Mankouri HW, Ashton TM, Hickson ID. Holliday junction-containing DNA structures persist in cells lacking Sgs1 or Top3 following exposure to DNA damage. Proc Natl Acad Sci U S A. 2011;108(12):4944-9. Epub 2011/03/09. doi: 10.1073/pnas.1014240108. PubMed PMID: 21383164; PubMed Central PMCID: PMCPMC3064375.

84. Bzymek M, Thayer NH, Oh SD, Kleckner N, Hunter N. Double Holliday junctions are intermediates of DNA break repair. Nature. 2010;464(7290):937-41. doi: 10.1038/nature08868. PubMed PMID: 20348905; PubMed Central PMCID: PMC20348905.

85. Cromie GA, Hyppa RW, Taylor AF, Zakharyevich K, Hunter N, Smith GR. Single Holliday junctions are intermediates of meiotic recombination. Cell. 2006;127(6):1167-78. Epub 2006/12/19. doi: S0092-8674(06)01466-8 [pii]

10.1016/j.cell.2006.09.050. PubMed PMID: 17174892; PubMed Central PMCID: PMC2803030.

86. Liberi G, Maffioletti G, Lucca C, Chiolo I, Baryshnikova A, Cotta-Ramusino C, et al. Rad51-dependent DNA structures accumulate at damaged replication forks in *sgs1* mutants defective in the yeast ortholog of BLM RecQ helicase. Genes Dev. 2005;19(3):339-50. Epub 2005/02/03. doi: 10.1101/gad.322605. PubMed PMID: 15687257; PubMed Central PMCID: PMCPMC546512.

87. Schwacha A, Kleckner N. Identification of double Holliday junctions as intermediates in meiotic recombination. Cell. 1995;83(5):783-91. PubMed PMID: 8521495; PubMed Central PMCID: PMC8521495.

88. San-Segundo PA, Clemente-Blanco A. Resolvases, Dissolvases, and Helicases in Homologous Recombination: Clearing the Road for Chromosome Segregation. Genes. 2020;11(1). Epub 2020/01/16. doi: 10.3390/genes11010071. PubMed PMID: 31936378; PubMed Central PMCID: PMCPMC7017083.

89. Attner MA, Miller MP, Ee LS, Elkin SK, Amon A. Polo kinase Cdc5 is a central regulator of meiosis I. Proc Natl Acad Sci U S A. 2013;110(35):14278-83. Epub 2013/08/07. doi: 10.1073/pnas.1311845110. PubMed PMID: 23918381; PubMed Central PMCID: PMCPMC3761645.

90. Argüello-Miranda O, Zagoriy I, Mengoli V, Rojas J, Jonak K, Oz T, et al. Casein Kinase 1 Coordinates Cohesin Cleavage, Gametogenesis, and Exit from M Phase in Meiosis II. Developmental Cell. 2017;40(1):37-52. doi: https://doi.org/10.1016/j.devcel.2016.11.021.

91. Geymonat M, Spanos A, Wells GP, Smerdon SJ, Sedgwick SG. Clb6/Cdc28 and Cdc14 regulate phosphorylation status and cellular localization of Swi6. Mol Cell Biol. 2004;24(6):2277-85. Epub 2004/03/03. PubMed PMID: 14993267; PubMed Central PMCID: PMCPMC355859.

92. Leem SH, Chung CN, Sunwoo Y, Araki H. Meiotic role of *SWI6* in *Saccharomyces cerevisiae*. Nucleic Acids Res. 1998;26(13):3154-8. Epub 1998/06/17. doi: gkb508 [pii]. PubMed PMID: 9628912; PubMed Central PMCID: PMC147675.

93. Kosugi S, Hasebe M, Tomita M, Yanagawa H. Systematic identification of cell cycle-dependent yeast nucleocytoplasmic shuttling proteins by prediction of composite motifs. Proc Natl Acad Sci U S A. 2009;106(25):10171-6. Epub 2009/06/13. doi: 10.1073/pnas.0900604106. PubMed PMID: 19520826; PubMed Central PMCID: PMCPMC2695404.

94. Talhaoui I, Bernal M, Mullen JR, Dorison H, Palancade B, Brill SJ, et al. Slx5-Slx8 ubiquitin ligase targets active pools of the Yen1 nuclease to limit crossover formation. Nat Commun. 2018;9(1):5016. Epub 2018/11/28. doi: 10.1038/s41467-018-07364-x. PubMed PMID: 30479332; PubMed Central PMCID: PMCPMC6258734.

95. Petes TD, Botstein D. Simple Mendelian inheritance of the reiterated ribosomal DNA of yeast. Proc Natl Acad Sci U S A. 1977;74(11):5091-5. Epub 1977/11/01. PubMed PMID: 337310; PubMed Central PMCID: PMCPMC432105.

96. Smith AV, Roeder GS. The yeast Red1 protein localizes to the cores of meiotic chromosomes. J Cell Biol. 1997;136(5):957-67. PubMed PMID: 9060462; PubMed Central PMCID: PMC2132480.

97. Vader G, Blitzblau HG, Tame MA, Falk JE, Curtin L, Hochwagen A. Protection of repetitive DNA borders from self-induced meiotic instability. Nature. 2011;477(7362):115-9. Epub 2011/08/09. doi: nature10331 [pii]

10.1038/nature10331. PubMed PMID: 21822291; PubMed Central PMCID: PMC3166416.

98. Herruzo E, Santos B, Freire R, Carballo JA, San-Segundo PA. Characterization of Pch2 localization determinants reveals a nucleolar-independent role in the meiotic recombination checkpoint. Chromosoma. 2019;128(3):297-316. Epub 2019/03/13. doi: 10.1007/s00412-019-00696-7. PubMed PMID: 30859296.

99. Pereira G, Manson C, Grindlay J, Schiebel E. Regulation of the Bfa1p-Bub2p complex at spindle pole bodies by the cell cycle phosphatase Cdc14p. J Cell Biol. 2002;157(3):367-79. Epub 2002/04/24. doi: 10.1083/jcb.200112085. PubMed PMID: 11970961; PubMed Central PMCID: PMCPMC2173300.

100. Pereira G, Schiebel E. Separase regulates INCENP-Aurora B anaphase spindle function through Cdc14. Science. 2003;302(5653):2120-4. Epub 2003/11/08. doi: 10.1126/science.1091936. PubMed PMID: 14605209.

101. Imtiaz A, Belyantseva IA, Beirl AJ, Fenollar-Ferrer C, Bashir R, Bukhari I, et al. *CDC14A* phosphatase is essential for hearing and male fertility in mouse and human. Human molecular genetics. 2018;27(5):780-98. Epub 2018/01/03. doi: 10.1093/hmg/ddx440. PubMed PMID: 29293958; PubMed Central PMCID: PMCPMC6059191.

102. Longtine MS, McKenzie A, 3rd, Demarini DJ, Shah NG, Wach A, Brachat A, et al. Additional modules for versatile and economical PCR-based gene deletion and modification in *Saccharomyces cerevisiae*. Yeast. 1998;14(10):953-61. Epub 1998/08/26. doi: 10.1002/(sici)1097-0061(199807)14:10<953::aid-yea293>3.0.co;2-u. PubMed PMID: 9717241.

103. Jaspersen SL, Charles JF, Tinker-Kulberg RL, Morgan DO. A late mitotic regulatory network controlling cyclin destruction in *Saccharomyces cerevisiae*. Mol Biol Cell. 1998;9(10):2803-17. Epub 1998/10/08. PubMed PMID: 9763445; PubMed Central PMCID: PMCPMC25555.

104. Padmore R, Cao L, Kleckner N. Temporal comparison of recombination and synaptonemal complex formation during meiosis in *S. cerevisiae*. Cell. 1991;66(6):1239-56. Epub 1991/09/20. doi: 0092-8674(91)90046-2 [pii]. PubMed PMID: 1913808.

105. Carballo JA, Panizza S, Serrentino ME, Johnson AL, Geymonat M, Borde V, et al. Budding yeast ATM/ATR control meiotic double-strand break (DSB) levels by down-regulating Rec114, an essential component of the DSB-machinery. PLoS Genet. 2013;9(6):e1003545. doi: 10.1371/journal.pgen.1003545. PubMed PMID: 23825959; PubMed Central PMCID: PMC23825959.

106. Ahuja JS, Borner GV. Analysis of meiotic recombination intermediates by two-dimensional gel electrophoresis. Methods Mol Biol. 2011;745:99-116. Epub 2011/06/11. doi: 10.1007/978-1-61779-129-1_7. PubMed PMID: 21660691.

107. Newnham L, Jordan PW, Carballo JA, Newcombe S, Hoffmann E. Ipl1/Aurora Kinase Suppresses S-CDK-Driven Spindle Formation during Prophase I to Ensure Chromosome Integrity during Meiosis. PLoS One. 2013;8(12):e83982. doi: 10.1371/journal.pone.0083982. PubMed PMID: 24386320; PubMed Central PMCID: PMC24386320.

Figure captions

Fig 1. *cdc14^{3HA}* behaves as a specific sporulation-deficient separation-of-function allele of *CDC14*. (A) The *cdc14^{3HA}* allele does not perturb normal growth conditions when cultivated at 25°C, 30°C and 37°C in rich media (YPD). (B) Homozygous SK1 *cdc14^{3HA}* diploids do not form asci containing spores under standard conditions for sporulation. (C) *cdc14^{3HA}* diploid cells divide mitotically but lack di-tyrosine autofluorescence induced by UV light upon several days incubation in SPM media at 30°C. (D) FACS analysis of DNA content shows that *cdc14^{3HA}* cells complete meiotic DNA replication with identical kinetics as *CDC14* diploid cells. (E) *cdc14^{3HA}* cells undergo meiotic nuclear divisions at subtly slower kinetics, and reduced frequencies, than *CDC14* cells. Error bars represent the SEM over the mean values plotted. (F) Di-tyrosine autofluorescence of different mutant combinations as well as the control strains grown and sporulated on plates at 25°C. *cdc14-1* homozygote diploids (JCY2353) sporulate at high efficiency under semi-permissive temperature forming preferentially tetrads whereas *cdc14^{3HA}* homozygote diploids (JCY840) do not sporulate. Combinations, and variable copy number, of the mutant genes can rescue the sporulation defect to different degrees (JCY2365/JCY2354/JCY2356).

Fig 2. Diminished Cdc14 protein levels in *cdc14^{3HA}* meiotic cells confer unsteady SPB integrity following meiotic divisions. (A) Analysis of Cdc14 protein levels in wild-type (JCY902), and *cdc14^{3HA}* (JCY904) cells. Top panel shows immunodetection using a polyclonal α-Cdc14 (yE-17) antibody. The same blot was reanalyzed using α-HA (12CA5) (bottom panel). (*) denotes residual signal from the earlier α-Cdc14 detection. *SMK1-3HA* is also expressed in both *CDC14* and *cdc14^{3HA}* strains. (B) Quantification of protein levels shown in (A). Values were normalized against the maximum signal corresponding to the 12 h time-point in the wild type. (C) Variability of protein levels in mitotic versus meiotic cells in different *CDC14* alleles. Exponentially growing cells show similar Cdc14 levels except for *cdc14^{3HA}*, which has lower overall protein levels (left panel). Direct comparison between the three alleles *CDC14* (JCY2232); *cdc14^{3HA}* (JCY2231) and *P_{CLB2}-3HA-CDC14* (JCY2389; *cdc14-md)* in exponentially growing mitotic cells (Exp.) and meiotic cultures immediately after they were transferred to SPM (Mei_0). Loading control for each lane was determined using Pgk1 protein levels. (D) Evolution of Cdc14 protein levels through meiosis in synchronous time-courses for *CDC14* (JCY2232), *cdc14^{3HA}* (JCY2231), and *cdc14-md* (JCY2389). Higher contrast was applied to visualize residual protein levels for all three alleles. Immunodetection of Pgk1 was used as loading control. FACS histograms for each time-point are depicted at the bottom to show the degree of synchrony reached in each culture. (E) Visualization of Spc29-CFP at SPBs, tubulin, and DNA, in wild-type (JCY892) and *cdc14^{3HA}* (JCY893) cells fixed at different stages of meiosis at 30°C. (F) *cdc14^{3HA}* cells develop meiosis I and II spindles with near wild-type kinetics. Lack of spore formation in *cdc14^{3HA}* meiotic cells parallels the loss of SPB's structural integrity.

Fig 3. Meiosis-deficient *cdc14^{3HA}* mutant does not alter meiotic spindle lifespan and dynamics. (A) Live-imaging of wild-type and *cdc14^{3HA}* cells (GGY53 and GGY54, respectively) undergoing the first meiotic division carrying GFP-tubulin (red) and Spc29-CFP (green). (B) Visualization of spindle and SPB dynamics in the same strains (GGY53 and GGY54) undergoing the second meiotic division. For both A and B, microscopy fields from at least four different positions and from two separate wells were analyzed. A minimum of three time-courses per strain were run, acquired images were processed and movies generated (Supplementary Information). (C) Quantification of spindle lifespan from cells undergoing MI or MII. Meiotic deficient *cdc14^{3HA}* cells (GGY54) show similar spindle dynamics compared to the wild type when completing both meiotic divisions. Box plots depict median number of spindle lifespan with whiskers representing upper and lower 1.5 interquartile range. Black dots represent outliers. Statistical test was performed using a two-tailed unpaired *t*-test. (D) Representative images of distinct morphological patterns for Rec8-GFP in meiosis. Full: bright nuclear localization. Diffuse: faint staining within the stretched nucleus. Peri: Rec8-GFP only visible at peri-centromeric locations. Absent: no Rec8-GFP signal. Pds1-tdTomato and CNM67-tdTomato were used to follow Pds1 accumulation/degradation and SPB number/location. (E) Example of meiotic cell transiting from prophase I to complete both meiotic divisions. Time 0 (min) was considered the last frame where Pds1 was visualized and SPBs stayed in close association. (F) Temporal distribution of the distinct morphological categories of Rec8-GFP shown in (D) for *CDC14* (JCY2406; n=57 cells) and *cdc14^{3HA}* (JCY2404; n=52 cells).

Fig 4. Missegregation of sister chromatids at MII in *cdc14^{3HA}* meiosis-deficient mutant cells. (A) Frequency of cells presenting connected DAPI masses at anaphase I in wild type (JCY902), *cdc14^{3HA}* (JCY904), *cdc14-md* (PRY132), *spo11* (PRY53) and *spo11 cdc14^{3HA}* (PRY55). **(B)** Frequency of cells presenting connected nuclei at metaphase II. Meiotic-deficient *cdc14^{3HA}* mutants (GGY54) present higher frequencies of unresolved nuclear divisions at late anaphase I and at metaphase II than wild type (GGY53). (C) Unequal distribution of homozygous chromosome II-linked GFP markers at *lys2* locus in meiosis-deficient *cdc14^{3HA}* mutant cells (JCY2330) denotes increased chromosome missegregation in comparison with wild-type cells (JCY2331). (D) Similar distribution of homozygous *CENIV*-linked GFP markers at *trp1* locus in meiosis-deficient *cdc14^{3HA}* mutant cells (JCY2286) in comparison with wild-type cells (JCY2284) denotes correct homolog disjunction in anaphase I. (E) Unequal distribution of heterozygous *CENIV-GFP* marker in meiosis-deficient *cdc14^{3HA}* tetranucleated mutant cells (JCY2327) denotes increased sister chromatid missegregation in comparison with wild-type cells (JCY2326). Statistical significance of differences was calculated by two-tailed *t*-test, assuming unequal variances ($^{*}p < 0.05$; $^{**}p < 0.01$; $^{***}p < 0.001$; $^{****}p < 0.0001$; n.s.: not significant). (F) Meiotic defects in

cdc14^{3HA} (JCY844) or *cdc14-md* (JCY2376) can be partly restored to wild-type levels (JCY840) by eliminating recombination (JCY2270/JCY2280/PRY151).

Fig 5. Analysis of meiotic recombination in meiotic-deficient *cdc14* mutants. (A) Schematic depiction of recombination analysis and intermediates at the *HIS4-LEU2* hotspot (see text in result sections for more details). (B) Representative 1D-gel Southern blot for analysis of DSBs and COs at the *HIS4-LEU2* hotspot using *XhoI* as the restriction site. Wild-type strain (JCY2232), *cdc14*^{3HA} (JCY2231), and *cdc14-md* (JCY2389). (C) Analysis of COs and NCOs at the *HIS4-LEU2* hotspot using *XhoI* and *NgoMVI* in the same strains as in (B). (D) Quantification of DSBs, COs and NCOs from the Southern blots shown in (B) and (C). (E) Comparison of the turnover of high molecular weight DNA species in *CDC14* (JCY2232) and *cdc14*^{3HA} (JCY2231) strains. (F) Representative 1D-gel Southern blot image for analysis of DSBs and COs at the *HIS4-LEU2* hotspot using *XhoI* in *CDC14 ndt80* strain (JCY2390) and *cdc14*^{3HA} *ndt80* (JCY2385) strains. (G) Analysis of COs and NCOs at the *HIS4-LEU2* hotspot using *XhoI* and *NgoMVI* in the same strains as in (F). (H) Quantification of DSBs, NCOs and JMs from the Southern blots shown in (F) and (G).

Fig 6. Analysis of recombination intermediates in *cdc14* mutants shows early and late accumulation of JMs. (A) Schematic representation of DNA species commonly observed after analysing the *HIS4-LEU2* hotspot by 2D-gel electrophoresis. (B) Representative Southern blots depicting 2D-gels at the *HIS4-LEU2* hotspot in *CDC14 ndt80* (JCY2390), *cdc14*^{3HA} *ndt80* (JCY2385) and *cdc14-md ndt80* (JCY2399) at two different times during meiosis. (C) Quantification of total JMs in the strains shown in (B) from several independent gels. Error bars display SEM over the mean values plotted (B). (D) Induction of *CDC5* in prophase-arrested *ndt80 mus81 cdc14*^{3HA} cells (JCY2440) leads to inefficient CO and NCO formation compared to *ndt80 mus81* (JCY2442). (E) Quantification of COs and NCOs from Southern blots shown in (D). (F) Representative Southern blots depicting 2D-gels at the *HIS4-LEU2* hotspot in *sgs1-md mms4* (JCY2444), *sgs1-md mms4 cdc14-md* (JCY2446) and *sgs1-md mms4 yen1* (JCY2448) 24 h into meiosis. (H) Quantification of total JMs in the strains shown in (F) from at least two independent gels. Error bars represent SEM over the calculated mean value. (G) Representative 1D-gel Southern blot images for analysis of crossovers at the *HIS4-LEU2* hotspot for all strains shown in (F) and for *cdc14-md* (JCY2389). (I) Quantification of COs from at least three different radioluminiscence digital image acquisitions like the one depicted in (G). Error bars represent SEM over the calculated mean value.

Fig 7. The absence of Cdc14 prevents activation of Yen1 during meiotic divisions. (A) Quantification of distinct localization patterns of Yen1 at meiosis I. (B) Analysis of expression levels and nuclease activity of Yen1 in *CDC14* (YJM7692) and *cdc14*^{3HA} (YML7693) meiotic cells. Soluble extracts were prepared from *YEN1-Myc9* strains at 2-hr intervals after transfer into sporulation medium

(SPM). Following anti-Myc immunoaffinity purification (IP), the IPs were analyzed by western blotting and tested for nuclease activity using Cy3-labeled Holliday junction DNA as a substrate. Upper panel: western blots of the cell extracts, with detection of Yen1-myc9, Cdc5, and Pgk1 (loading control). Lower panel: HJ resolution assay. The experiment shown is representative of two independent experiments. (C) Percentage of HJ cleavage in Yen1 IPs in the presence or absence of Cdc14 meiotic activity. (D) Evolution of DNA content during meiosis from strains in (B). (E) Unrestrained resolution of recombination intermediates by Yen1^{ON} improves sporulation in *cdc14^{3HA}* (JCY2164) and *cdc14-md* (PRY182) cells. Frequency of asci containing one, two, three and four spores in the strains of the indicated genotypes. (F) Frequency of cells presenting connected DAPI masses at anaphase I (left panel) or sister chromatid missegregation (right panel) in *YEN1^{ON}* (PRY123/PRY99), *cdc14^{3HA}* (JCY2327/PRY55) and *cdc14^{3HA} YEN1^{ON}* (PRY121/PRY108). (G) Deficient HJ resolution in *cdc14^{3HA}* (YML7693) is efficiently restored by the presence of Yen1^{ON} (JCY2421). Western blot analysis of Yen1/Yen1^{ON} immunoprecipitates is shown on the left panels. HJ resolution assay is shown on the right panel. Quantification of resolution efficiency is displayed at the bottom. Resolution data arise from two independent experiments.

Fig 8. Model for *CDC14*-dependent resolution of complex recombination intermediates via multiple mechanisms. Contribution of Cdc14 to the correct disjunction of recombining chromosomes during meiosis. Early in prophase I, chromosomes initiate homologous recombination. 3'-resected ssDNA overhangs invade an intact template with the help of recombinases. Displacement of the intact strand from the template allows the formation of D-loops, which can be stabilized allowing DNA synthesis. Next, stabilized branched DNA molecules might be disrupted by the action of the anti-recombinase heterotrimeric complex STR (Sgs1-Top3-Rmi1). Reannealing of the extended 3'-ssDNA overhang with the resected complementary strand, followed by further DNA synthesis will lead to the repair and ligation of the broken DNA duplex, giving rise to a NCO via SDSA. The second end of the DSB can engage with the sister-chromatid at random leading to the formation of multi-chromatid JMs. Cdc14 prevents the accumulation of JMs by an unknown mechanism. ZMM stabilization of JMs is followed by the resolution of dHJs through the MutLγ, class I, CO pathway. Ndt80-dependent expression, and activation, of Cdc5 triggers MutLγ resolvase activity. Unresolved linkages between bivalents that persist until anaphase I are mostly resolved by the action of the SSEs, Mus81-Mms4. Slx1-Slx4, Top3-Rmi1 as well as Cdc14 also contribute to the correct resolution of chromosomal entanglements between homologs during MI by unknown mechanisms. Residual chromatid intertwining between sister chromatids during the second meiotic division will be removed by the action of Yen1. The resolvase has been kept previously inactive by inhibitory phosphorylations until the second release of Cdc14 during anaphase II that dephosphorylates the resolvase promoting its full activation. See discussion for more details.

Supporting information captions

S1 Fig. Cdc14 is required during meiosis for correct nuclear division. (A) *cdc14*^{3HA} cells (JCY844) sustain both nuclear divisions although with subtly slower kinetics than wild type cells (JCY840) predominantly during the second round of nuclear segregation. *cdc14-md* cells (JCY2376) do not undergo the second nuclear division (B) Quantification of the number of nuclei as well as other aberrant nuclear structures during meiosis in *CDC14* (JCY840) and *cdc14*^{3HA} (JCY844) cells. (C) Representative images of all nuclear structures described in (B).

S2 Fig. Reduced levels of Cdc14 causes the sporulation defect observed in the *cdc14*^{3HA} mutant. (A) Sporulation efficiency of *cdc14*^{3HA} diploids transformed with multi-copy plasmids carrying MEN genes (GGY102/GGY103/GGY104/GGY105) and *cdc14*^{3HA} (GGY93). Only overproduction of the Cdc14 phosphatase rescues the sporulation defect. (B) Di-tyrosine autofluorescence of different mutant combinations as well as the control strains grown and sporulated on plates at 25ºC and 30ºC. *cdc14-1* homozygote diploids (JCY2353) sporulate at high efficiency under semi-permissive temperature forming preferentially tetrads whereas *cdc14*^{3HA} homozygote diploids will not sporulate at any temperature (JCY840). Combinations, and variable copy number, of the mutant genes can rescue the sporulation defect at different degrees (JCY2365/JCY2354/JCY2356).

S3 Fig. Meiotic *cdc14* mutant cells re-duplicate their SPBs and assemble both meiosis I, and II, spindles. (A) Representative images of fixed cells at different time-points during synchronous parallel time courses for both *CDC14* (JCY892) and *cdc14* mutant (JCY893) cells. *cdc14*^{3HA} cells initiate both meiotic divisions, as visualized by different fluorescence markers, but they do not complete sporulation. (B) *cdc14*^{3HA} (JCY893) cells display abnormal number of SPBs and atypical spindle conformations. (C) Terminal phenotype of a post-meiotic *cdc14*^{3HA} (JCY893) cell. (D) *cdc14-md* cells display strong SPB re-duplication defects and arrest with two nuclei.

S4 Fig. Lack of Cdc14 in meiosis causes missegregation of chromosomes at both meiotic divisions. (A) Scheme depicting the chromosome GFP-tagging system placed at an interstitial *locus* within chromosome II. (B) Representative images and frequencies of the observed types of distribution of interstitial GFP dots in homozygosis of both *cdc14*^{3HA} mutant (JCY2230) and wild-type (JCY2231) meiotic cells. Cells were fixed in formaldehyde and nuclei stained with DAPI. Arrowheads indicate diffuse GFP in the nucleus. Bar=5µm.

S5 Fig. Lack of Cdc14 in meiosis causes missegregation of centromeres following both meiotic divisions. (A) Scheme depicting the chromosome GFP-tagging system placed at a centromere proximal *locus* within chromosome IV. (B) Representative images and frequencies of the observed types of distribution of interstitial GFP dots in homozygosis of both *cdc14*^{3HA} mutant (JCY2330) and wild-type (JCY2331) meiotic cells. Cells were fixed in formaldehyde and nuclei stained with DAPI. Bar=5µm.

S6 Fig. Lack of Cdc14 and Mus81 causes problems in recombination. (A) Quantification of DNA species from Fig 6B. Error bars represent standard errors. (B) Representative 2D gels showing recombination intermediates in *ndt80, mus81 ndt80*, and *mus81 cdc14*^{3HA} *ndt80* prophase-arrested cells 8 h after meiotic induction. (C) Quantification of DNA species from (B). (D) Comparison of JM abundance and resolution from the Southern blot shown in (Fig 6D). Asterisk indicates meiosis-specific non-characterized recombination products.

S7 Fig. Precursors of spores are normally assembled and expressed in the absence of Cdc14 (A) Representative images displaying the circular appearance of the pro-spore membrane component Don1-GFP following completion of both meiotic divisions in *cdc14*^{3HA} mutant (JCY904) and wild-type (JCY902) cells. (B) Western blot showing the kinetics of meiotic production of the protein Ssp1 in wild-type (JCY840) and *cdc14*^{3HA} mutant (JCY844) cells. Ssp1 is a subunit of the leading edge protein (LEP) complex (Ssp1-Ady3-Don1-Irc10) that establishes a ring-like structure at the leading edge of the prospore membrane at MII and is required for spore formation. (C) Western blot analysis of the MAP Kinase Smk1, becoming highly phosphorylated in meiosis in both *cdc14*^{3HA} mutant (JCY904) and wild-type (JCY902) cells, which is representative of proficient sporulation potential.

S1 Table. *S. cerevisiae* strains used in this study. SK1 background strains were used throughout the study, unless specified otherwise.

S1 Video. Meiotic spindle lifespan and dynamics in *CDC14* cells. Live imaging of cells (GGY53) undergoing both meiotic division carrying GFP-tubulin (red) and Spc29-CFP (green).

S2 Video. Meiotic spindle lifespan and dynamics in *cdc14*^{3HA} cells. Live imaging of cells (GGY54) undergoing both meiotic division carrying GFP-tubulin (red) and Spc29-CFP (green).

S3 Video. Kinetics of Rec8-GFP association/removal in *CDC14* cells. Sequence of Rec8-GFP wild-type cells (JCY2406) at 15 minutes interval displaying kinetics of cohesins assembly and removal.

S4 Video. Kinetics of Rec8-GFP association/removal in *cdc14*^{3HA} cells. Sequence of Rec8-GFP *cdc14*^{3HA} cells (JCY2404) at 15 minutes interval displaying kinetics of cohesins removal.

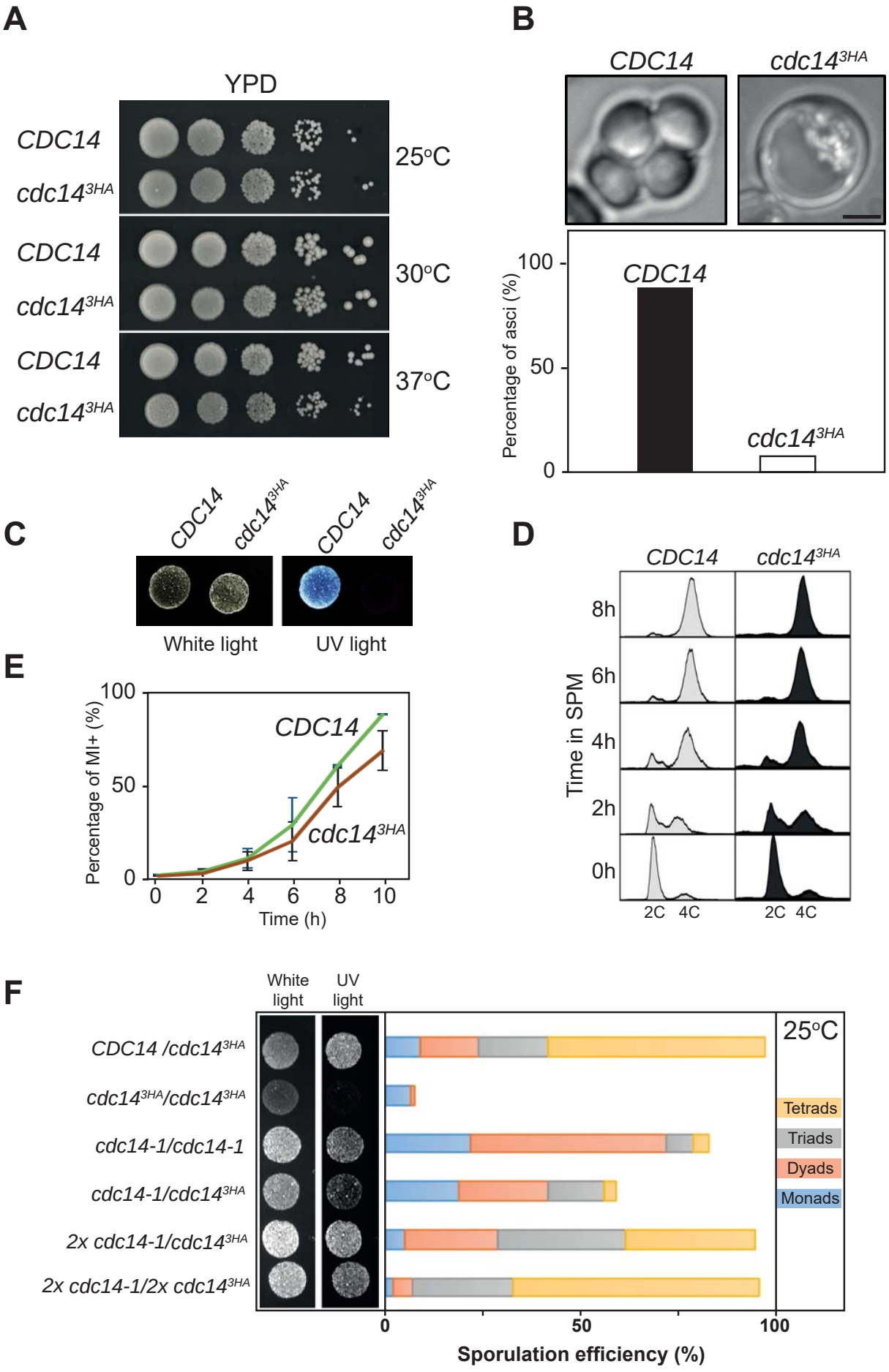

Figure 2

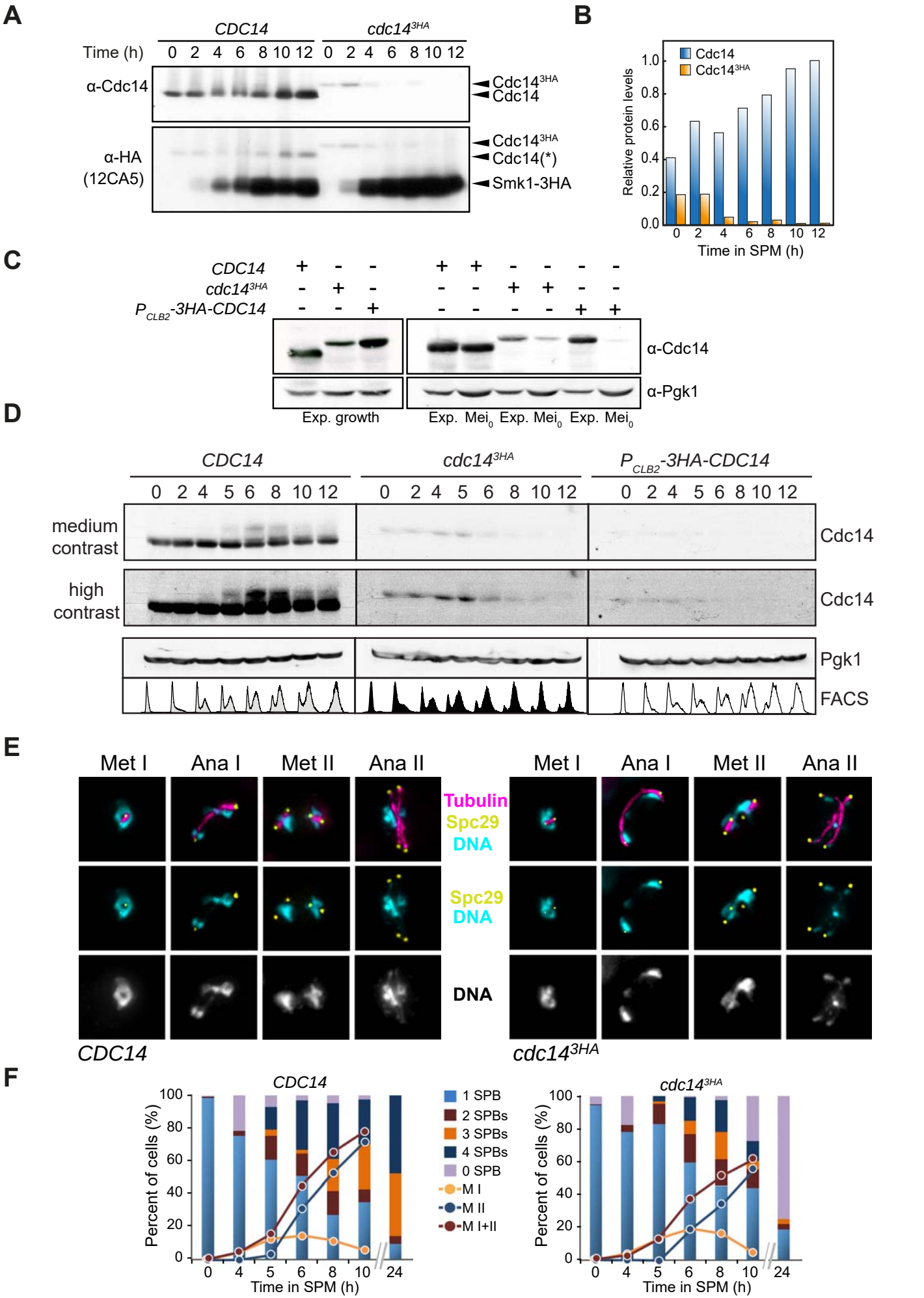

Figure 3

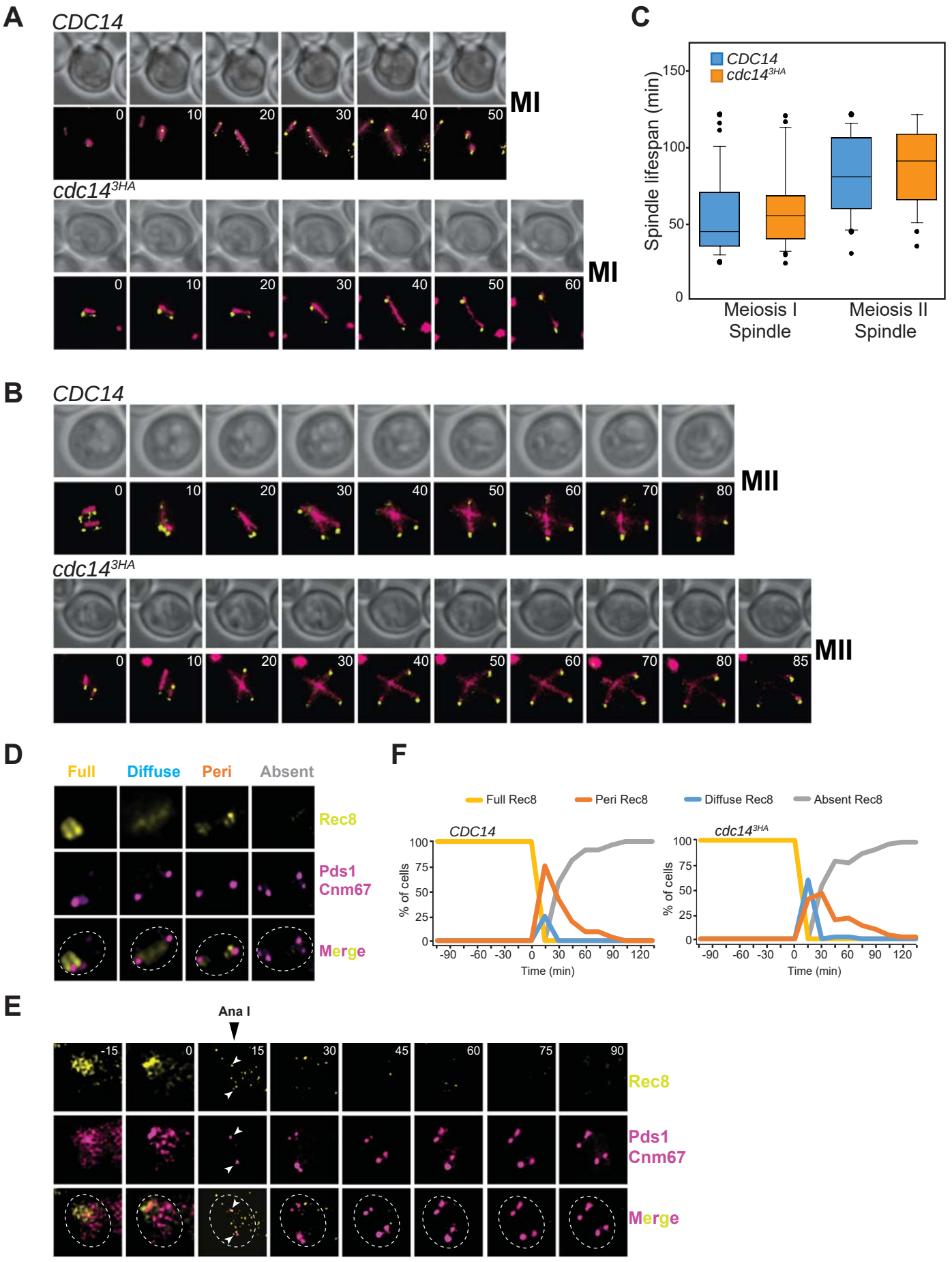

Figure 4

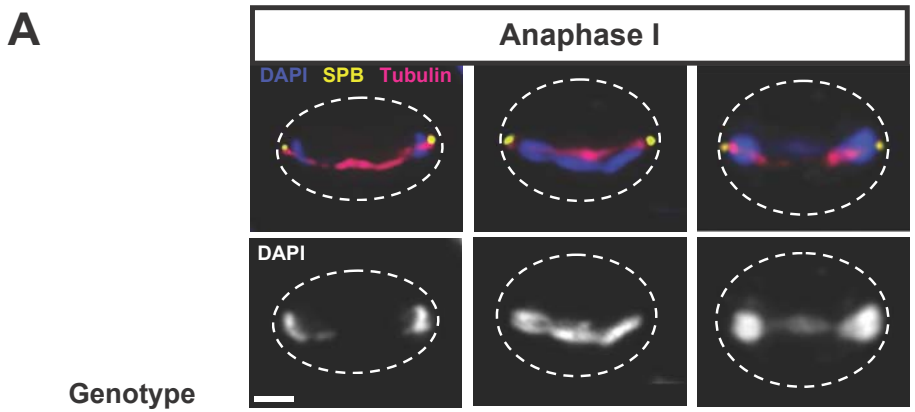

Genotype			
WT	74.3%	22.6%	3.1%
cdc14^{3HA}	19.6%	67.3%	13.1%
P$_{CLB2}$CDC14	20.5%	71.1%	8.4%
spo11	77.1%	20.0%	2.9%
spo11 cdc14^{3HA}	61.4%	34.5%	4.1%

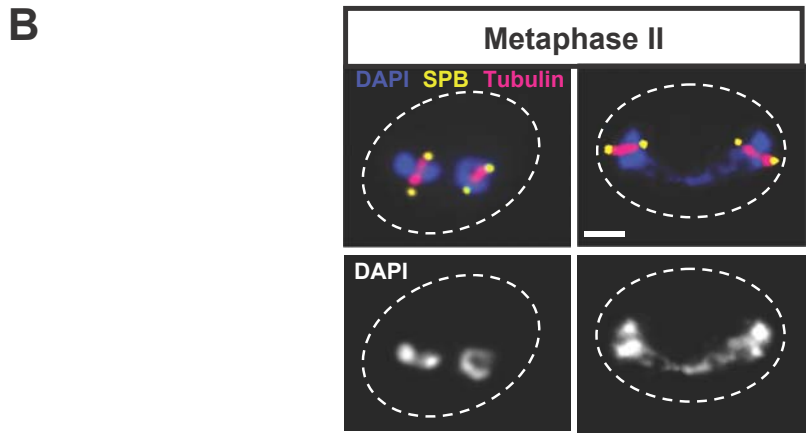

WT	76.3%	24.7%
cdc14^{3HA}	24.6%	75.3%

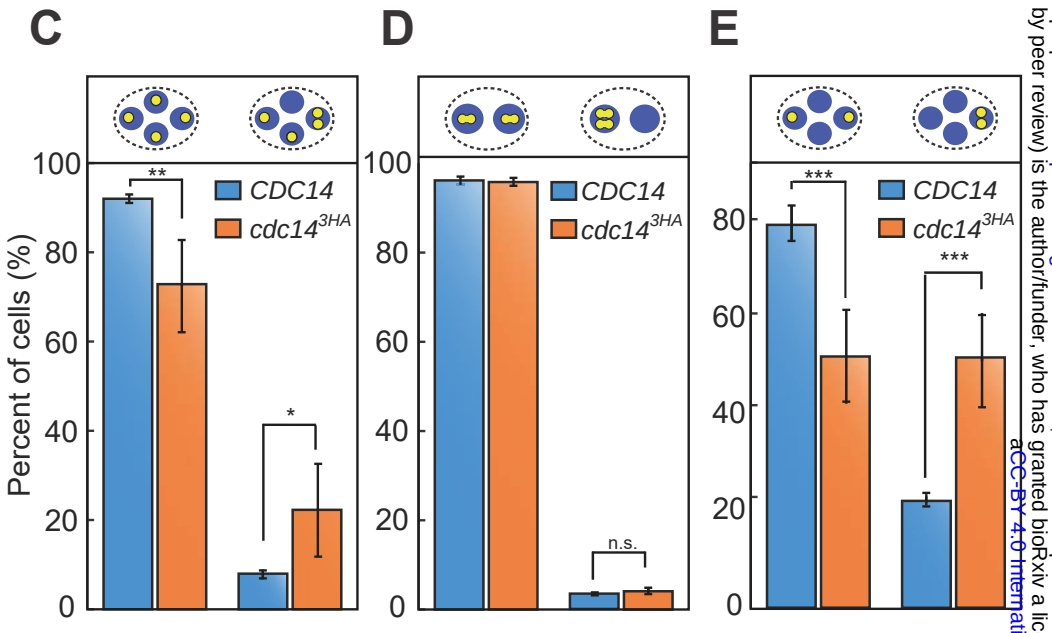

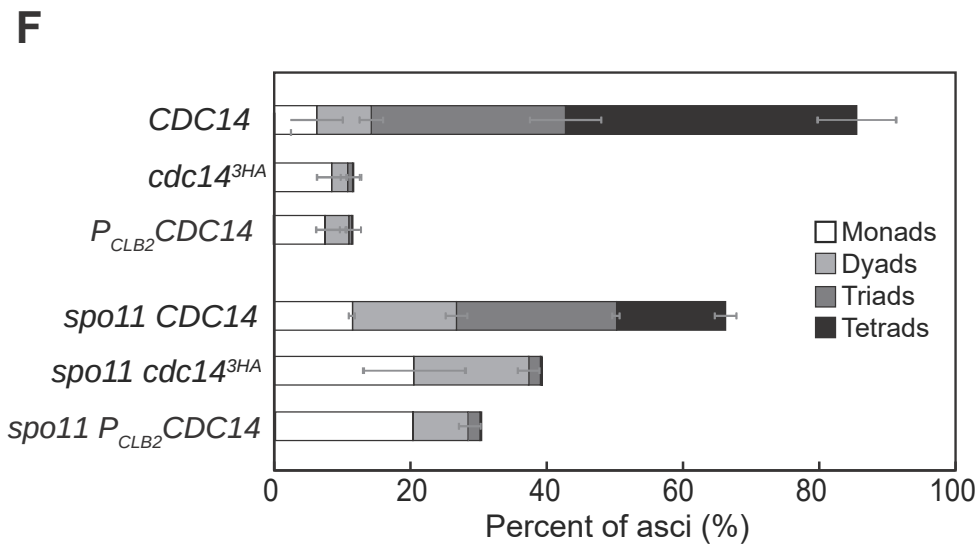

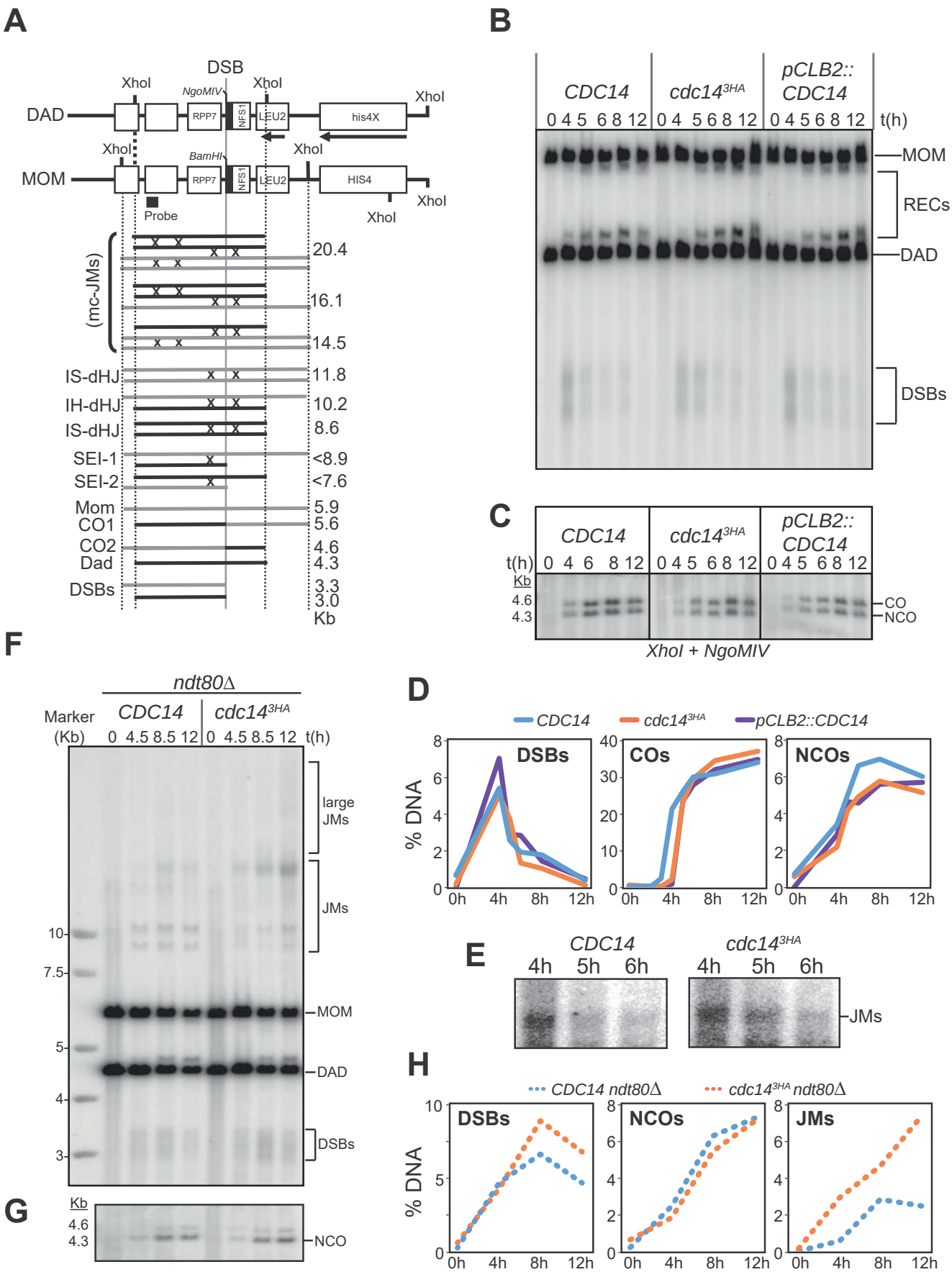

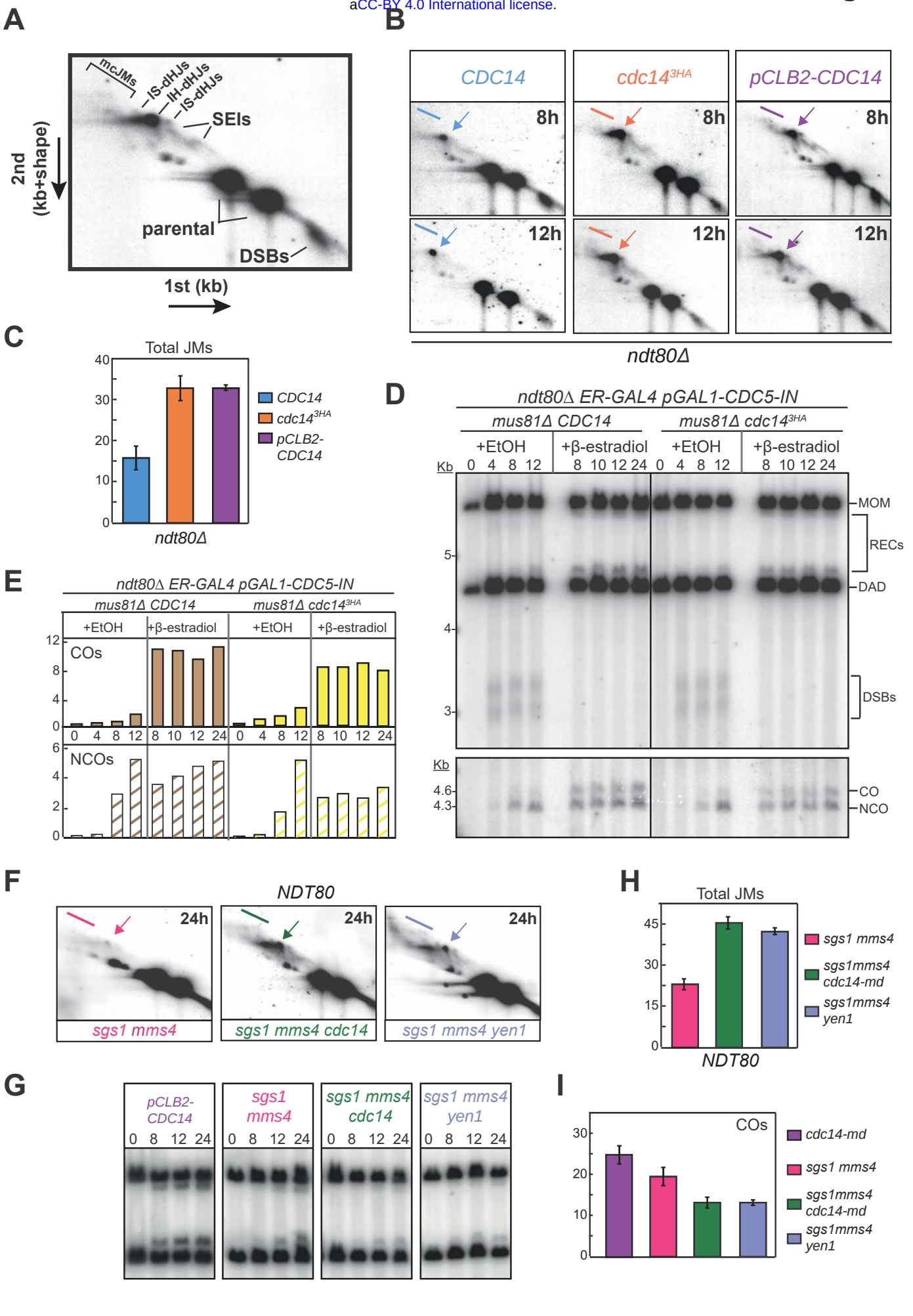

A

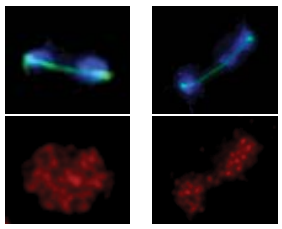

	Pan [%]	Nuclear [%]
CDC14	48	52
cdc14^{3HA}	81	19

B

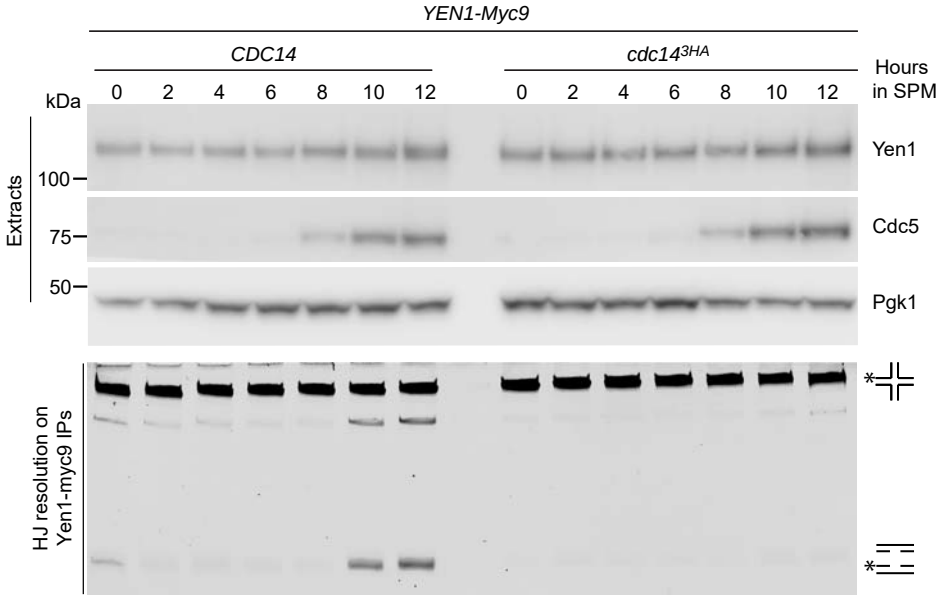

C

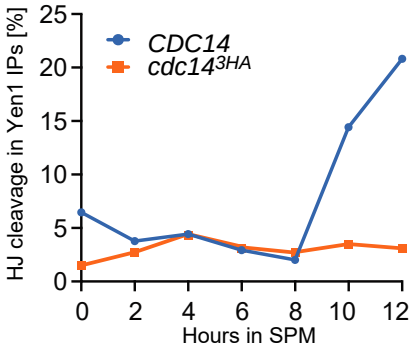

D

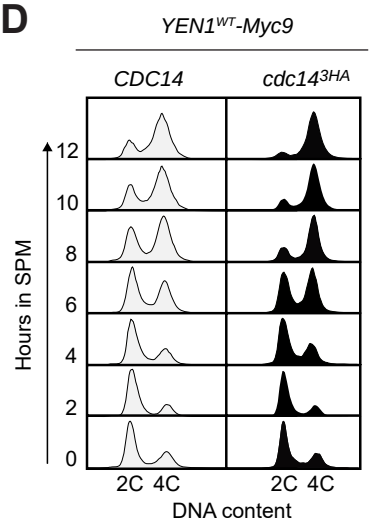

E

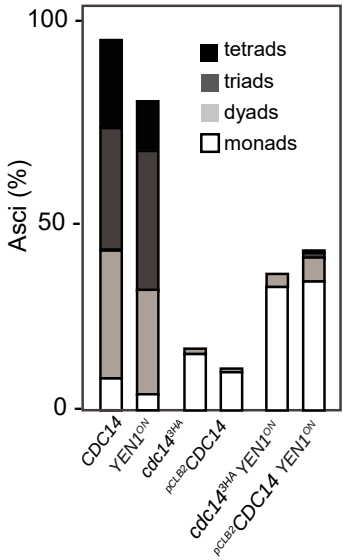

F

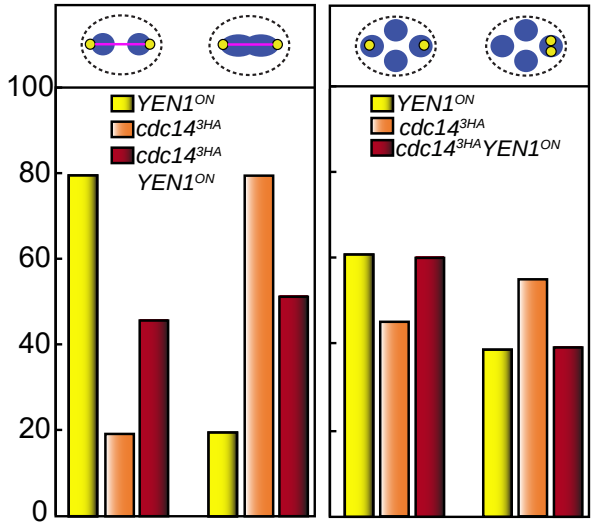

G

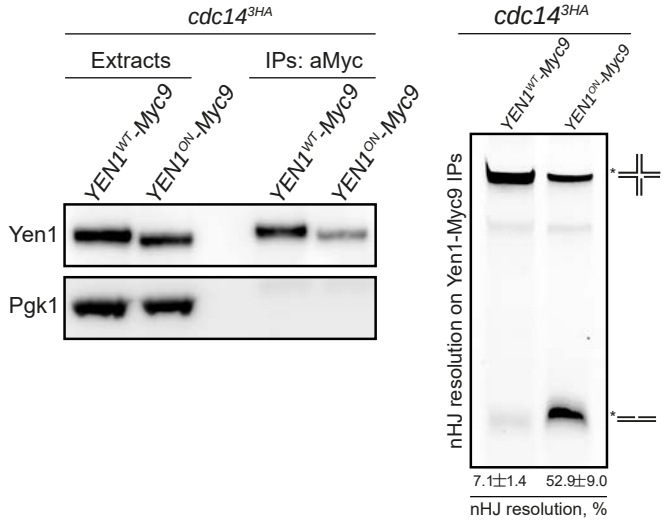

Figure 8

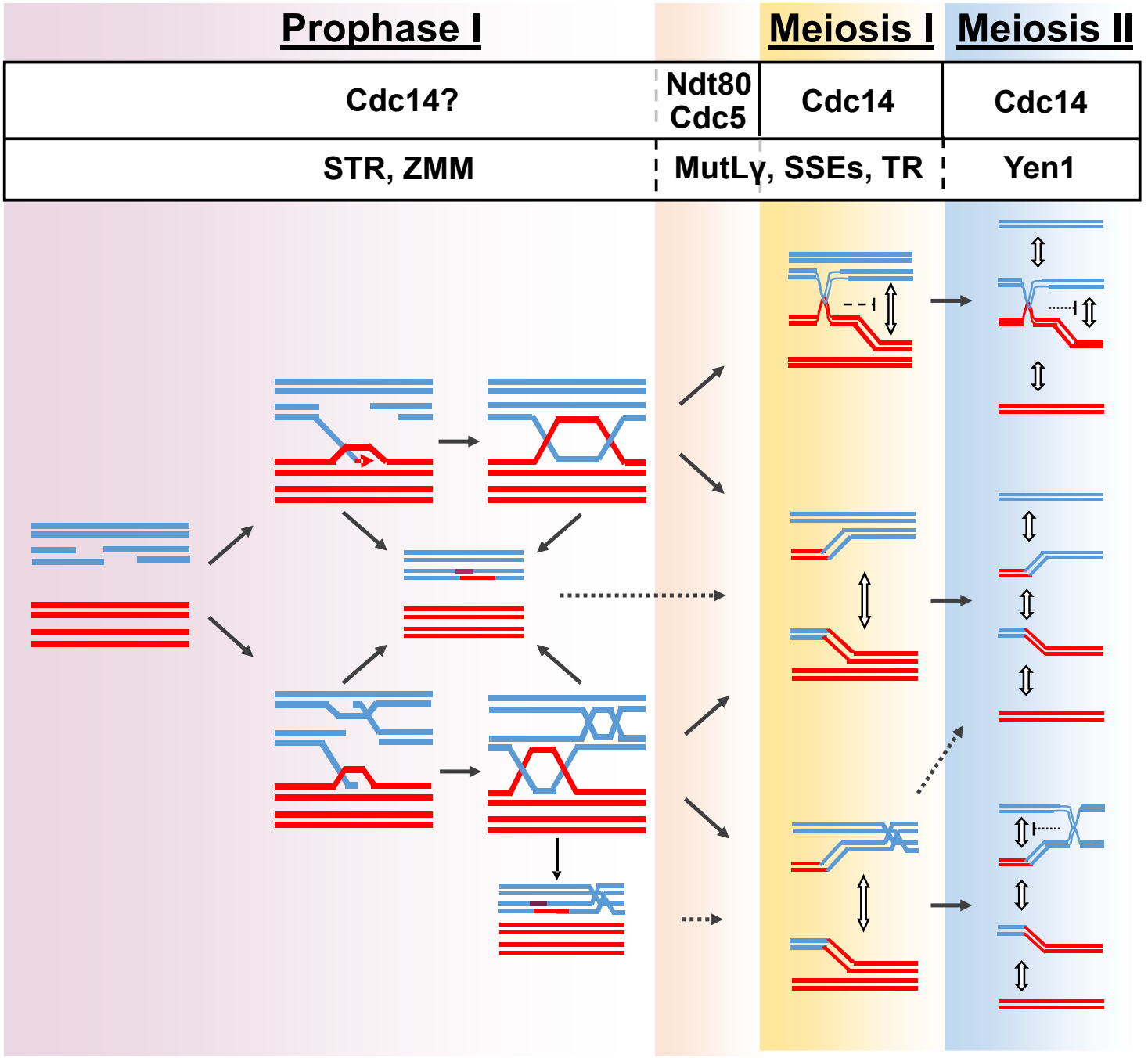

S1 Table. *S. cerevisiae* strains used in this study

Strain	Genotype
JCY840	*MAT a/α ho::LYS2/", lys2/", ura3/", leu2::hisG/", trp1::hisG/", arg4-nsp/", his4x/"*
JCY844	*MAT a/α ho::LYS2/", lys2/", ura3/", leu2::hisG/", trp1::hisG/", arg4-nsp/", his4x/", cdc14^{3HA}::KanMX4/"*
GGY92	*MAT a/α ho::hisG/LYS2, lys2, ura3(Dsma-pst::hisG)/ura3, HIS4::LEU2-(NBam;ori)/his4x, Zip1-GFP(at AA700)/", leu2::hisG/", cdc14^{3HA}::KanMX4/CDC14*
GGY91	*MAT a/α ho::hisG/LYS2, lys2, ura3(Dsma-pst::hisG)/ura3, HIS4::LEU2-(NBam;ori)/his4X or LEU2(NgomIV;ori)-URA3/his4x, Zip1-GFP(at AA700), leu2::hisG/", cdc14^{3HA}::KanMX4/"*
JCY902	*MAT a/α ho::hisG/", ura3/", leu2::hisG/+, lys2/", trp1/", SPC29-CFP::TRP1/", DON1-dGFP-KanMX/", pSMK1-3HA-URA3*
JCY904	As JCY902 but *cdc14^{3HA}::KanMX4/"*
GGY53	*MAT a/α ho::hisG/", ura3/", leu2::hisG/+, lys2/", trp1/", SPC29-CFP::TRP1/", TUB-dGFP-URA3/"*
GGY54	*MAT a/α ho::hisG/", ura3/", leu2::hisG/+, lys2/", trp1/", SPC29-CFP::TRP1/", TUB-dGFP-URA3/", cdc14^{3HA}::KanMX4/"*
JCY2196	*MAT a/α ho::hisG/", lys2/", ura3/", trp1/", his4/", leu2::hisG/", cdc14^{3HA}::KanMX4/"*
PRY151	*MAT a/α ho::LYS2/", lys2/", ura3/", leu2::hisG/", trp1::hisG/", spo11-Y135F-HA::URA3/", pCLB2::3HA-CDC14::KanMX4/"*
JCY2247	As JCY2235 but *cdc14^{3HA}::KanMX4/"*
JCY2270	*MAT a/α ho::LYS2/", lys2/", leu2::hisG/", ura3/", arg4-nsp/", trp1::hisG/", his4x/", spo11-Y135F-HA::URA3/"*
JCY2280	As JCY2270 but *cdc14^{3HA}::KanMX4/"*
JCY2232	*MAT a/α ho::hisG/", lys2/", ura3(Δsma-pst::hisG)/", leu2::hisG/", his4X::LEU2-(NgoMIV;ori)-URA3/HIS4::LEU2-(NBam;ori)*
JCY2231	As JCY2232 but *cdc14^{3HA}::KanMX4/"*
YJM7692	*MAT a/α ho::LYS2/" ura3/" leu2::hisG/" trp1::hisG/" his3::hisG/" YEN1-myc9::URA3/"*
YML7693	As YML3952 but *cdc14^{3HA}::KanMX4/"*

JCY2164	*MAT a/α ho::LYS2/", lys2/", ura3/", leu2::hisG/", trp1/", his4x::LEU2-URA3/", YEN1-9A-myc18::URA3/", cdc14^{3HA}::KanMX4/", ZIP1-eGFP(at AA700)/"*
GGY102	JCY844 with pSJ103 (*CDC15HA3-URA3)*
GGY93	JCY844 with pPD.2 (*CDC14HA3-URA3)*
GGY104	JCY844 with pSJ56 (*TEM1HA3-URA3*)
GGY105	JCY844 with pSJ29 (*HACDC5-URA3*)
JCY2353	*MAT a/α ho::LYS2/", lys2/", his4x/", leu2::hisG/", ura3/", cdc14Δ::KanMX4/", trp1::cdc14-1::TRP1::LEU2/"*
JCY2365	*MAT a/α ho::LYS2/", lys2/", his4x/", leu2::hisG/", ura3/", cdc14Δ::KanMX4/CDC14^{3HA}::KanMX4, trp1::cdc14-1::TRP1::LEU2/trp1 arg4-nsp/ARG4*
JCY2354	*MAT a/α ho::LYS2/", lys2/", his4x/", leu2::hisG/", ura3/", cdc14^{3HA}::KanMX4/cdc14Δ::KanMX4, trp1::cdc14-1::TRP1::LEU2/"*
JCY2356	*MAT a/α ho::LYS2/", lys2/", his4x/", leu2::hisG/", ura3/", cdc14^{3HA}::KanMX4/cdc14^{3HA}::KanMX4, trp1::cdc14-1::TRP1::LEU2/"*
JCY2222	*MAT a/α ho::LYS2/", lys2/", ura3/", leu2::hisG/", his4/", Cyc1p-LacI-GFP-URA3/", trp1::LacO-TRP1 (at CENIV)/"*
JCY2224	As JCY2222 but *cdc14^{3HA}::KanMX4/"*
JCY2284	*MAT a/α ho::LYS2/", lys2/", ura3/", leu2::hisG/", his4/", Cyc1p-LacI-GFP-URA3/ura3, trp1::LacO-TRP1 (at CENIV)/trp1*
JCY2286	As JCY2284 but *cdc14^{3HA}::KanMX4/"*
JCY2251	*MAT a/α ho::LYS2/", his4/", trp1/", lys2::TetOx240:URA3/lys2, leu2::LEU2 tetR-GFP/leu2*
JCY2248	As JCY2251 but *cdc14^{3HA}::KanMX4/"*
JCY2331	*MAT a/α ho::LYS2/", his4/", trp1/", lys2::TetOx240:URA3/", leu2::LEU2 tetR-GFP/", CNM67-mCherry::natMX4/CNM67*
JCY2330	As JCY2331 but *cdc14^{3HA}::KanMX4/"*
PRY53	*MAT a/α ho::LYS2/", leu::hisG/", spo11-Y135F-HA::URA3/",TUB-dGFP-URA3/", SPC29-CFP::TRP1/"; HIS4X/hisx4x*
PRY55	*MAT a/α ho::LYS2/", leu::hisG/", spo11-Y135F-HA::URA3/",TUB-dGFP-URA3/", SPC29-CFP::TRP1/", cdc14^{3HA}::KanMX4/", arg4/", HIS4/his4x*

PRY99	*MAT a/α ho::LYS2/'', leu2/'', his4x/'', trp1-ura3/LacO-TRP1 (at CENIV))-Cyc1p-LacI-GFP-URA3, YEN1-9A/''*
PRY108	*MAT a/α ho::LYS2/'', leu2/'', his4x/'', trp1-ura3/LacO-TRP1 (at CENIV)-Cyc1p-LacI-GFP-URA3, cdc14^{3HA}::KanMX4/'', YEN1-9A/''*
PRY121	*MAT a/α ho::LYS/'', leu2/'', SPC29-CFP::TRP1/'', YEN1-9A/'', TUB-dGFP-URA3/'', his3/'', cdc14^{3HA}::KanMX/''*
PRY123	*MAT a/α ho::LYS/'', leu2/'', SPC29-CFP::TRP1/'', YEN1-9A/'', TUB-dGFP-URA3/'', his3/''*
PRY132	*MAT a/α ho::LYS2/ho::hisG, lys2/'', leu2::hisG/'', TUB-dGFP-URA3/'', SPC29-CFP::TRP1/'', pCLB2:3HA-CDC14::KanMX4/'', his3/''*
JCY2389	*MAT a/α ho::hisG/'', lys2/'', ura3(Δsma-pst::hisG)/'', leu2::hisG/'', his4X::LEU2-(NgoMIV;ori)-URA3/HIS4::LEU2-(NBam;ori), pCLB2::3HA-CDC14::KanMX4/''*
JCY2385	*MAT a/α ho::hisG/'', lys2/'', ura3(Δsma-pst::hisG)/'', leu2::hisG/'', his4X::LEU2-(NgoMIV;ori)-URA3/HIS4::LEU2-(NBam;ori), ndt80::hphMX6/'', cdc14^{3HA}::KanMX4/''*
JCY2390	*MAT a/α ho::hisG/'', lys2/'', ura3(Δsma-pst::hisG)/'', leu2::hisG/'', his4X::LEU2-(NgoMIV;ori)-URA3/HIS4::LEU2-(NBam;ori), ndt80::hphMX6/''*
JCY2399	*MAT a/α ho::hisG/'', lys2/'', ura3(Δsma-pst::hisG)/'', leu2::hisG/'', his4X::LEU2-(NgoMIV;ori)-URA3/HIS4::LEU2-(NBam;ori), ndt80::hphMX6/'', pCLB2::3HA-CDC14::KanMX4/''*
JCY2440	*MAT a/α ho::hisG/'', lys2/'', ura3(Δsma-pst::hisG)/'', leu2::hisG/'', his4X::LEU2-(NgoMIV;ori)-URA3/HIS4::LEU2-(NBam;ori), ndt80::hphMX6/'', mus81::hphMX4/'', cdc14^{3HA}::KanMX4/'', pCDC5-Gal4-ER-pGAL1-CDC5-natMX4/''*
JCY2442	*MAT a/α ho::hisG/'', lys2/'', ura3(Δsma-pst::hisG)/'', leu2::hisG/'', his4X::LEU2-(NgoMIV;ori)-URA3/HIS4::LEU2-(NBam;ori), ndt80::hphMX6/'', mus81::hphMX4/'' pCDC5-Gal4-ER-pGAL1-CDC5-natMX4/''*
JCY2444	*MAT a/α ho::hisG/'', lys2/'', ura3(Δsma-pst::hisG)/'', leu2::hisG/'', his4X::LEU2-(NgoMIV;ori)-URA3/HIS4::LEU2-(NBam;ori), mms4::hphMX6/'', pCLB2::3HA-SGS1::KanMX4/''*
JCY2446	As JCY2444 but *pCLB2::3HA-CDC14::KanMX4/''*
JCY2448	As JCY2444 but *yen1::natMX4/''*
JCY2421	*MATa/α ho::LYS2/'' ura3/'' leu2::hisG/'' trp1::hisG/'' his3::hisG/'' YEN1-9A-myc18::URA3/''*

S1 Table

JCY2406	*MATa/α ho::LYS2/" ura3/" leu2::hisG/" trp1::hisG/" his3::hisG/" REC8-GFP::LEU2::KanMX4/", PDS1-tdTomato::KiTRP1/", CNM67-tdTomato::NatMX4/"*
JCY2404	As JCY2406 but *cdc14^{3HA}::KanMX4/"*

S1 Fig

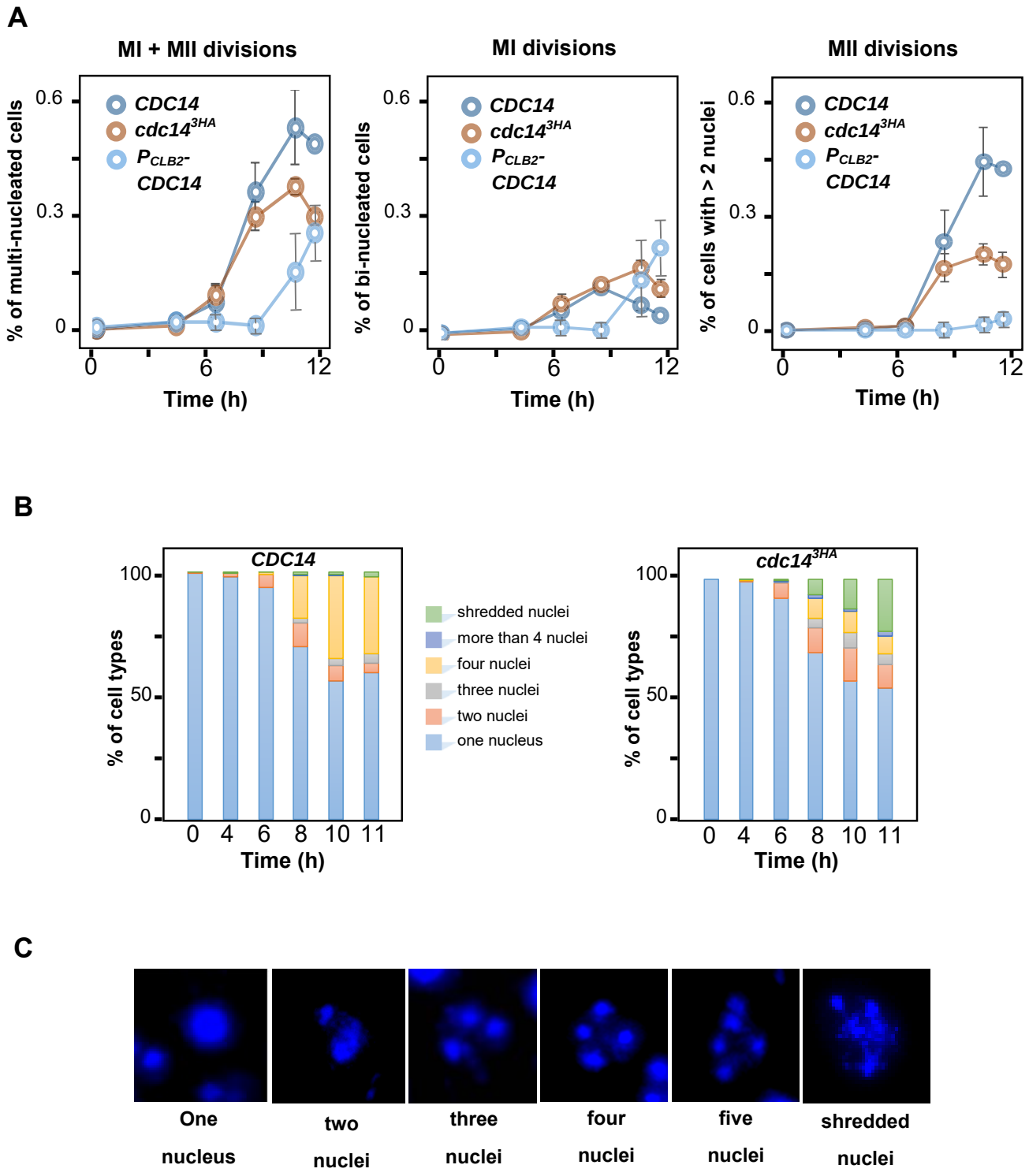

A

Genotype	Sp. Efficiency
cdc14^{3HA} + 2µm (empty)	10.0%
cdc14^{3HA} + OX (*cdc14*^{3HA})	32.4%
cdc14^{3HA} + OX (*TEM1*^{3HA})	5.0%
cdc14^{3HA} + OX (*HA-CDC5*)	8.0%
cdc14^{3HA} + OX (*3HA-DBF2*)	7.6%
cdc14^{3HA} + OX (*CDC15*^{3HA})	10.6%
CDC14 + 2µm (empty)	62.8%

B

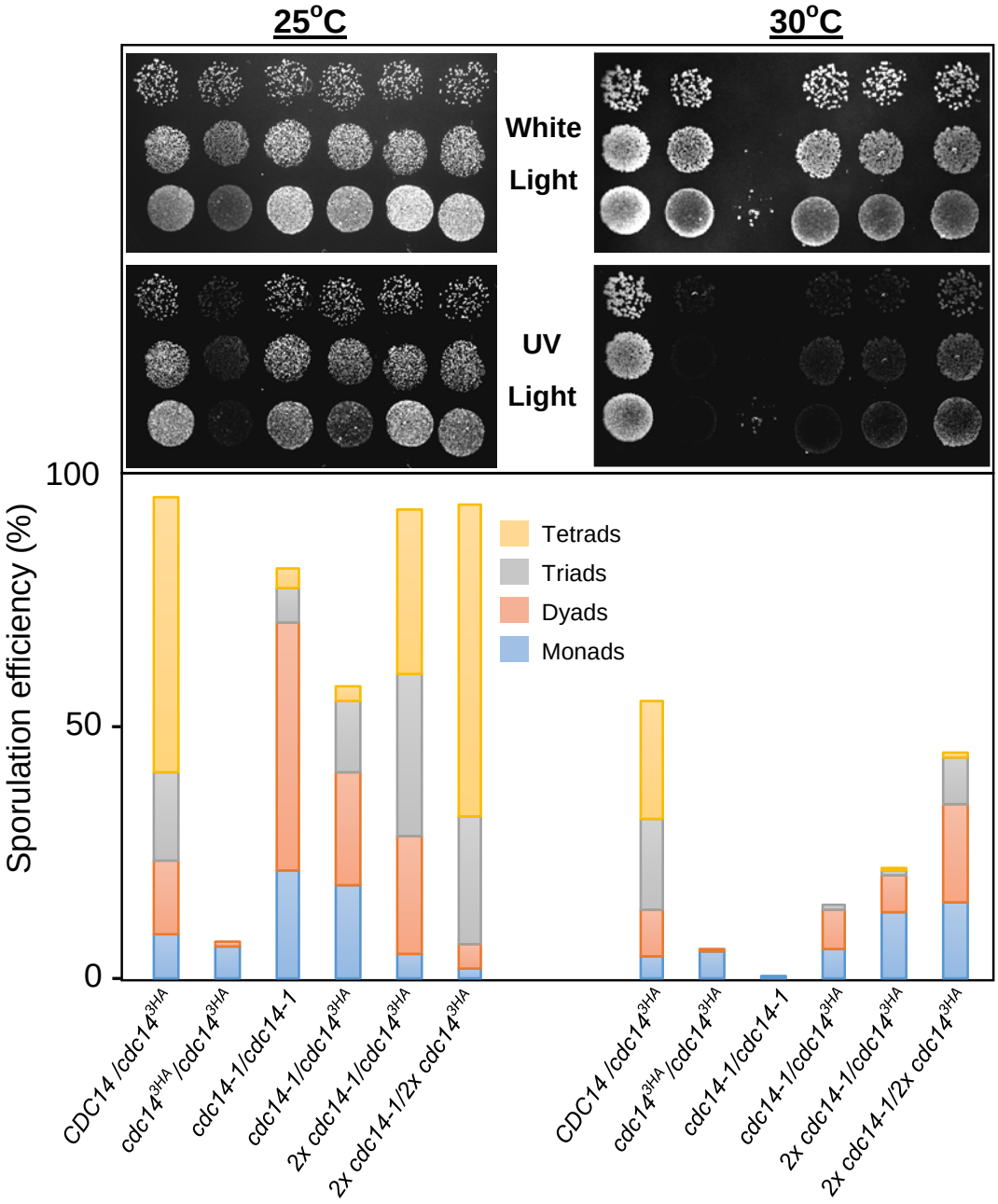

S3 Fig

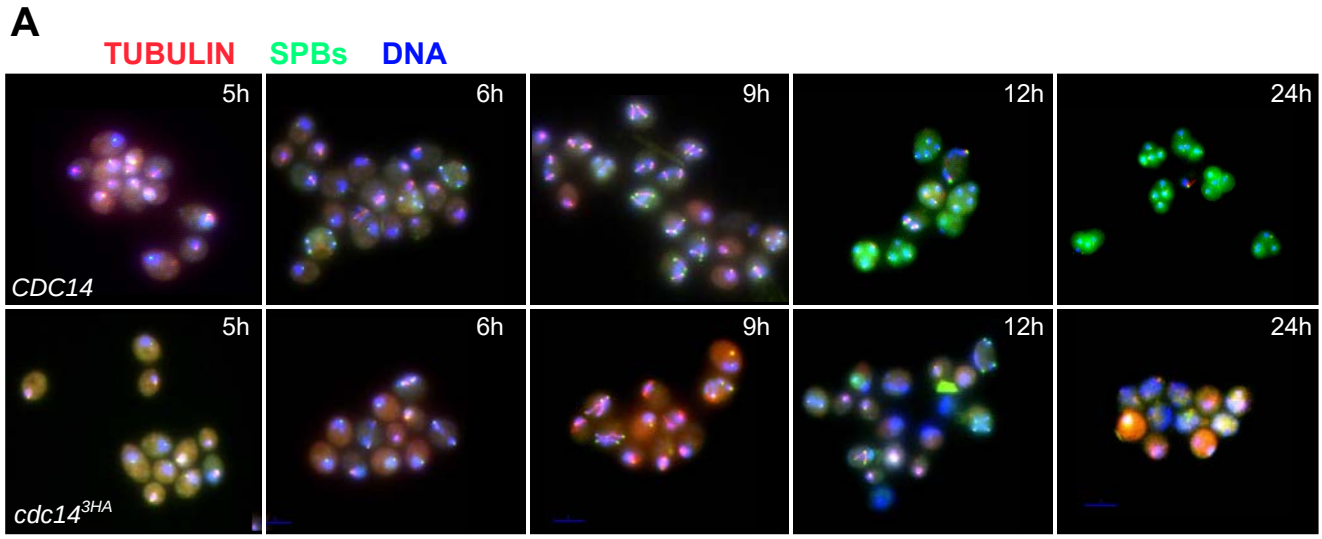

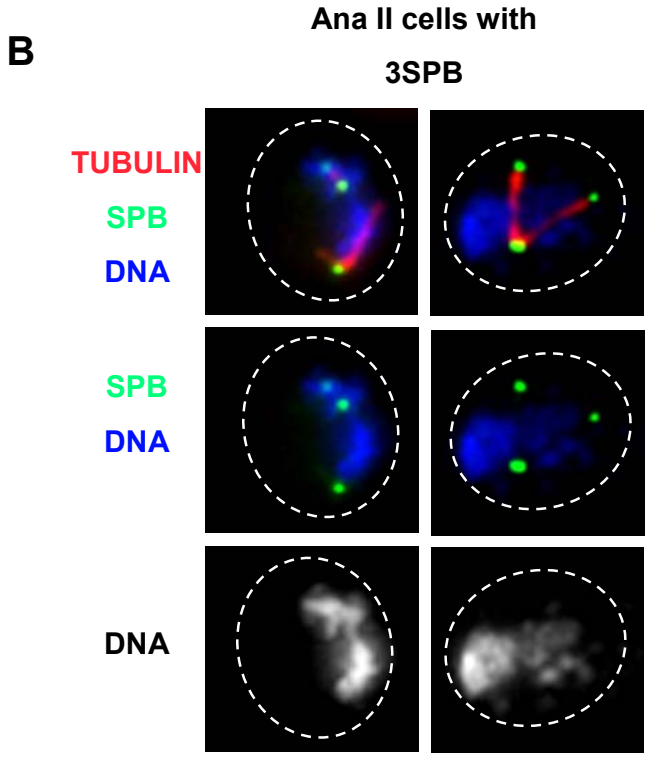

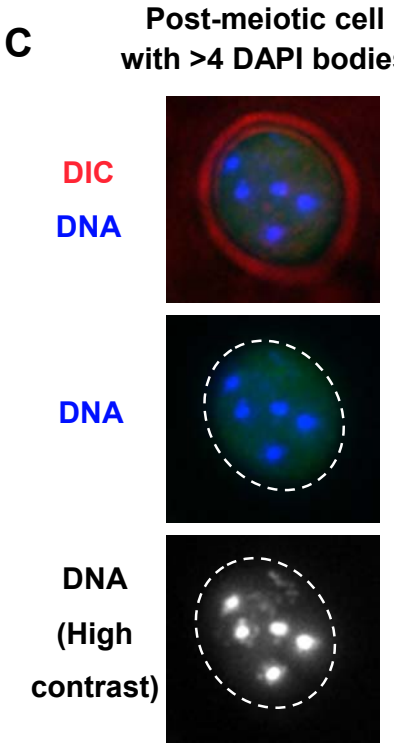

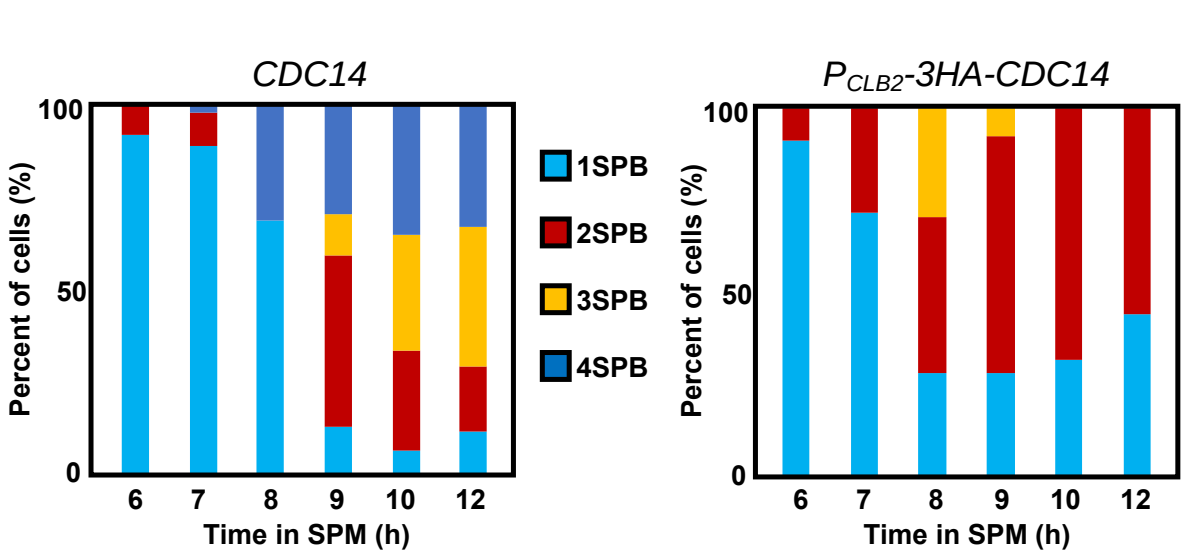

S4 Fig

A

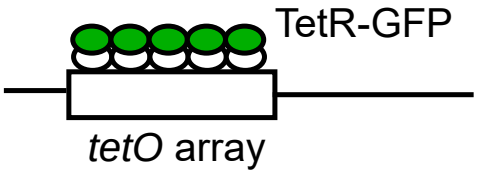

B

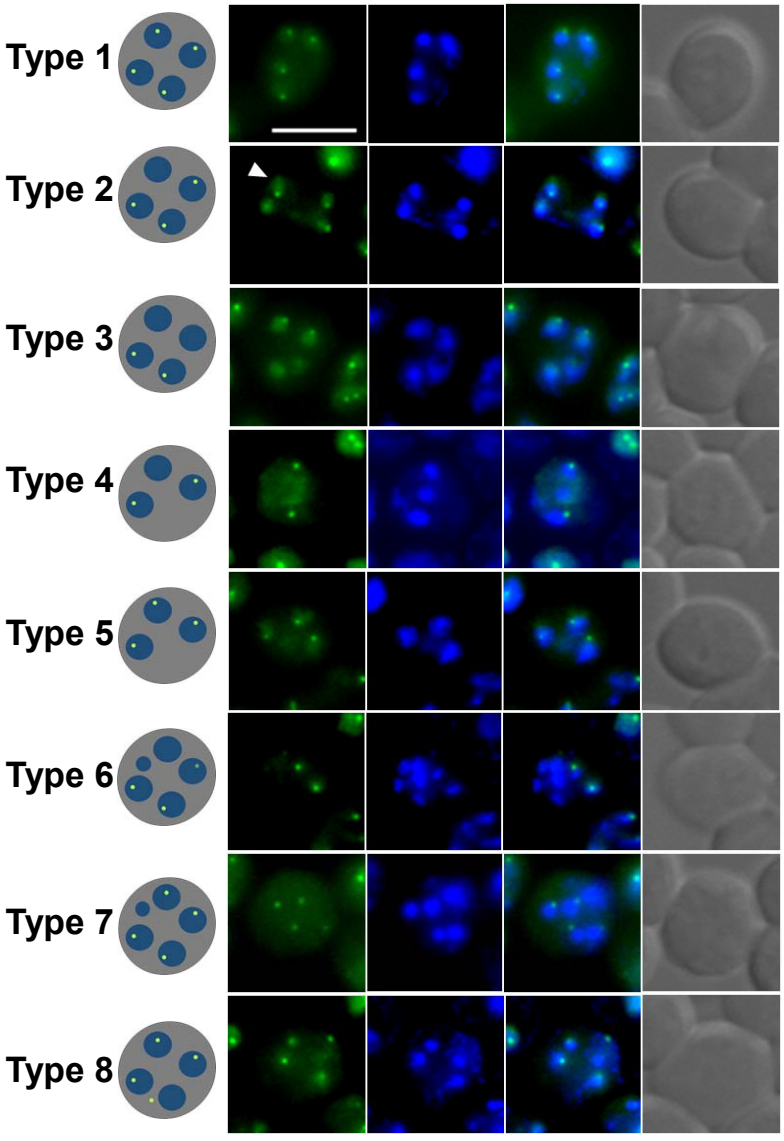

ChrII (*lys2*)

	CDC14	*cdc14*^{3HA}
Type 1	92.0%	42.4%
Type 2	2.4%	8.5%
Type 3	2.1%	3.3%
Type 4	0.3%	5.7%
Type 5	1.4%	13.2%
Type 6	0.3%	5.7%
Type 7	1.0%	14.5%
Type 8	0.5%	6.7%

S5 Fig

A

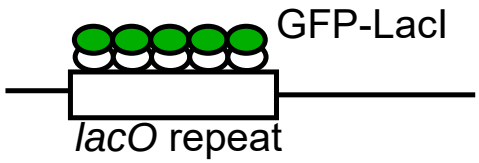

B

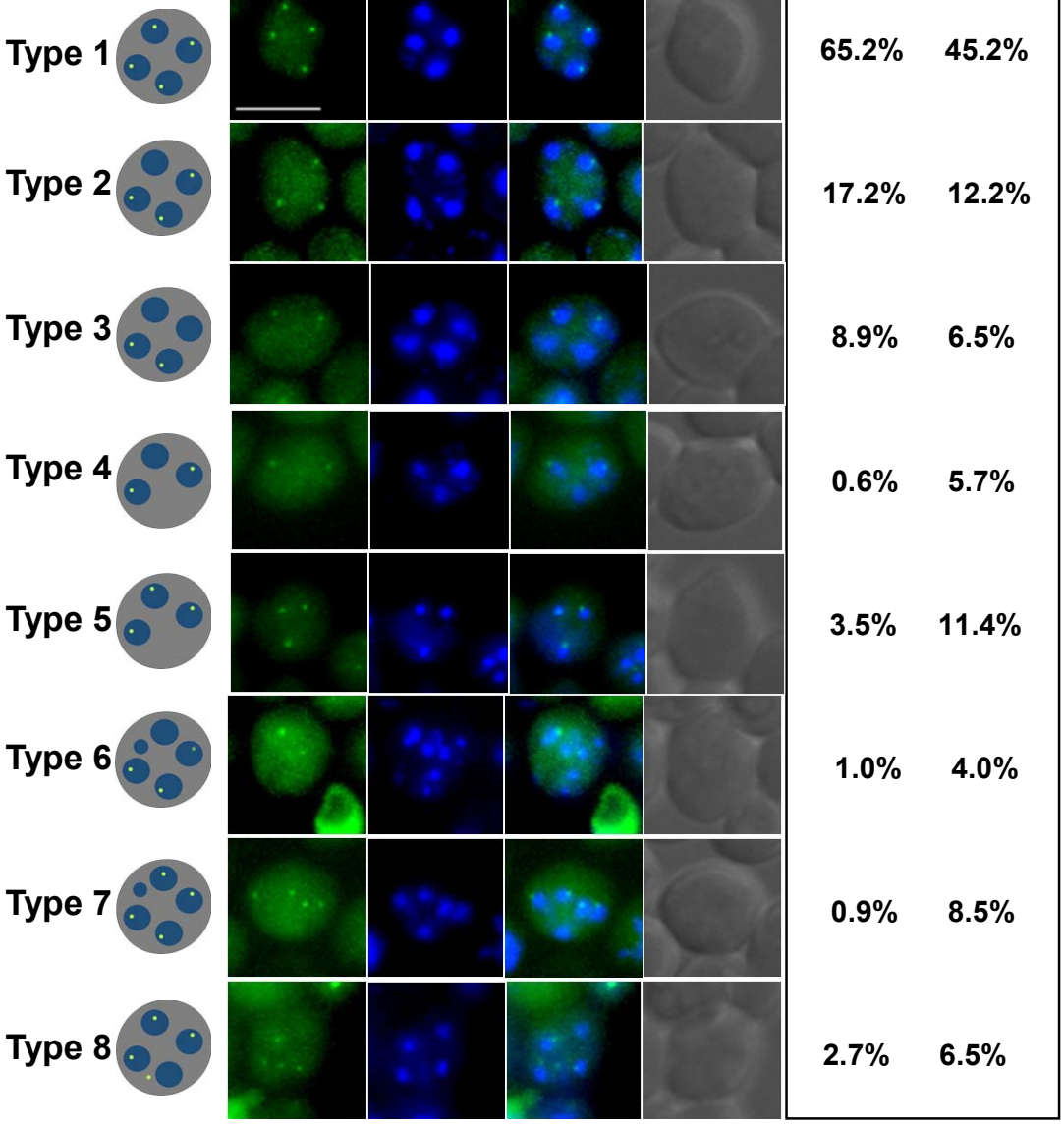

A

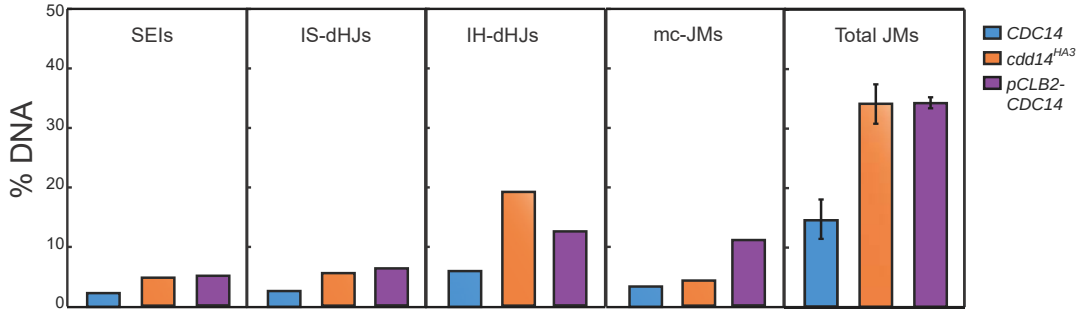

B

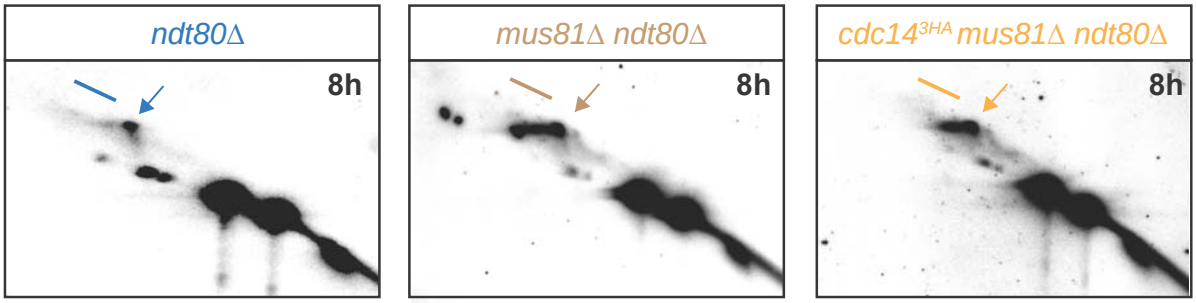

C

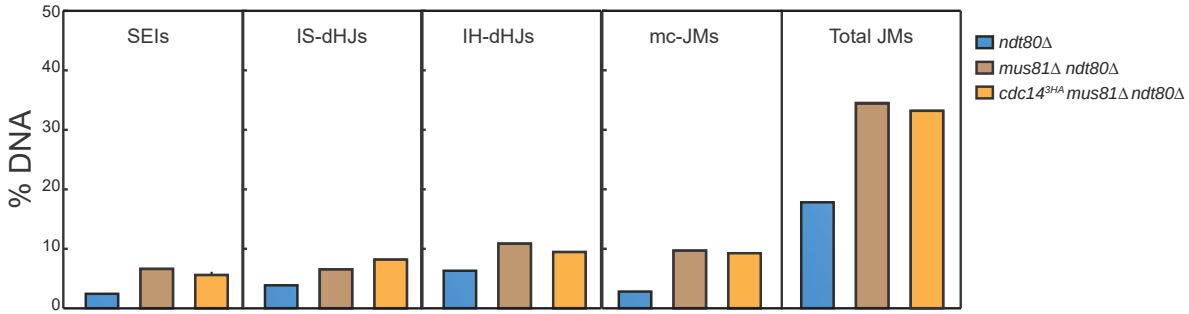

D

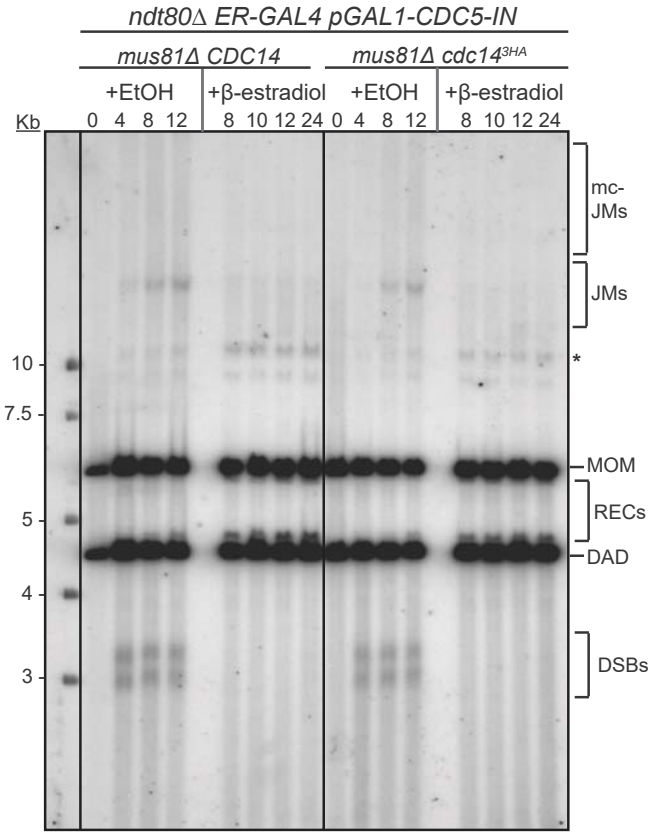

A

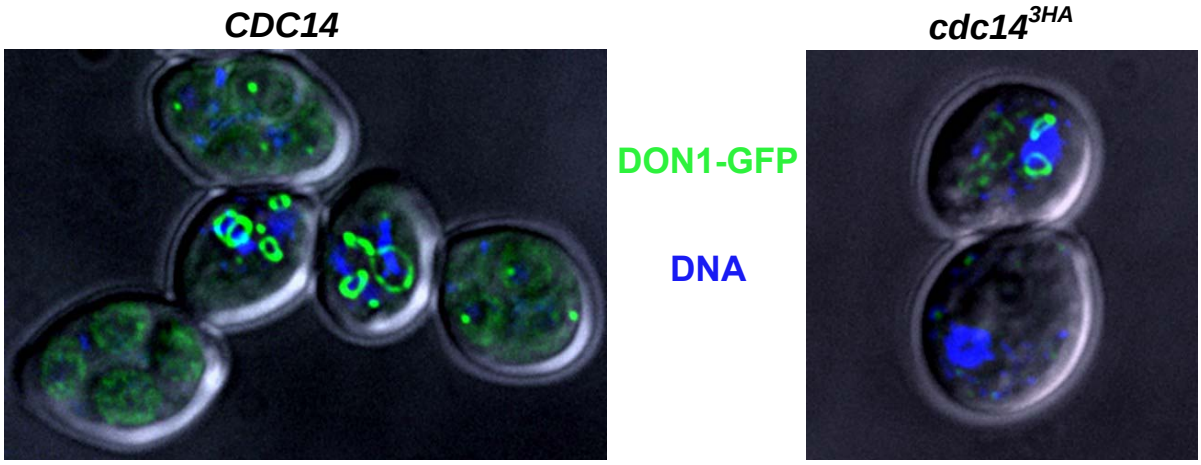

B

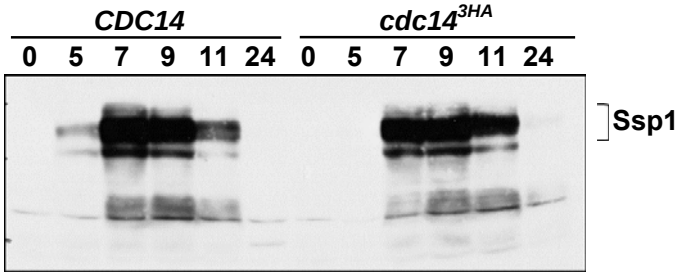

C